Data in brief: Conceptual design-optimisation of a subsonic hydrogen-powered long-range blended-wing-body aircraft

Swapnil S. Jagtap [a,*], Peter R.N. Childs [b] and Marc E.J. Stettler [a]

[a] Department of Civil and Environmental Engineering, Imperial College London, London SW7 2AZ, United Kingdom

[b] Energy Futures Lab, Imperial College London, London SW7 2AZ, United Kingdom

* Corresponding author: swapniljagtap111@gmail.com

Abstract:

This is additional data to the main paper publication

Link to the main paper:

https://www.sciencedirect.com/science/article/pii/S0360319924050225

Nomenclature

AR	Aspect ratio	OML	Outer mould line
BWB	Blended wing body	PAX	Passengers
C_{D}	Drag coefficient	RoC	rate of climb
$C_{\mathrm{D,0}}$	Coefficient of zero-lift drag	S	Wing area
C_{f}	Skin friction coefficient	SEC	Specific energy consumption
C_{L}	Coefficient of lift	SLS	Sea level static
e	Oswald's efficiency factor	SPK	Synthetic paraffin kerosene
FF	Fuel fraction	S_{wet}	Aircraft wetted area
GTF	Geared turbofan	TOC	Top of climb
GTOW	Gross take-off weight	TSFC	Thrust specific fuel consumption
HCDstruct	Hybrid wing body Conceptual Design and structural optimisation	t/c	Thickness to chord ratio
LH_2	Liquid hydrogen	T/W	Thrust to weight ratio
LNG	Liquid natural gas	UHB	Ultra-high bypass ratio
LTA	Large twin aisle	V	Airspeed
L/D	Lift to drag ratio	VLTA	Very large twin aisle
MTOW	Maximum take-off weight	W_{aircraft}	Aircraft weight
$M_{ff,climb}$	Climb fuel fraction	$W_{\mathrm{F,block}}$	Block fuel weight
$M_{ff,cruise}$	Cruise fuel fraction	$W_{\mathrm{F,total}}$	Total fuel weight carried at mission start
$M_{ff,loiter}$	Loiter fuel fraction	η	Gravimetric index
OEW	Operating empty weight	ρ_a	Air density

SI 1. Review of conceptual aircraft design process

The initial stage of the aircraft design process is called 'conceptual design process' and 'preliminary sizing' by Raymer [1] and Roskam [2], respectively. In most cases, conceptual design begins with specific design requirements. These are set by company-generated models, market research/survey, or by the prospective customer, towards the future needs of the customers. The design requirements comprise parameters such as aircraft range, payload, speed requirements, etc. for civil or military applications. Figure SI 1 depicts the conceptual design process in more detail. In some cases, a design may be initiated as an innovative idea instead of a response to a given requirement. For example the aircraft project called 'flying wings' was not conceived in response to a requirement. It was a product of Northrop's idea of a 'better airplane.' Before initiating a new aircraft design, a decision has to be made as to what technologies will be used depending on the timeframe in which the aircraft is expected to enter in service [1,3].

The effort for conceptual design begins with a conceptual sketch. This is a rough illustration of what the design might look like. A good conceptual sketch will include the approximate geometries, shape, and locations of the major aircraft components. The conceptual sketch may be used to evaluate the weight fractions and aerodynamics by comparing it to prior designs. These approximate evaluations are helpful for providing a first estimate of the necessary fuel weight and total weight for performing a designed mission, by a process known as 'sizing.' The conceptual sketch might not be even required for the initial sizing if the design resembles a prior design. The initial sizing gives the specific data required for developing an initial design layout, which is a three-view engineering drawing completed with geometries, shapes, and locations of the major aircraft components, and any other internal components that are large enough to affect the overall shaping of the aircraft. It is used to verify that everything fits [1].

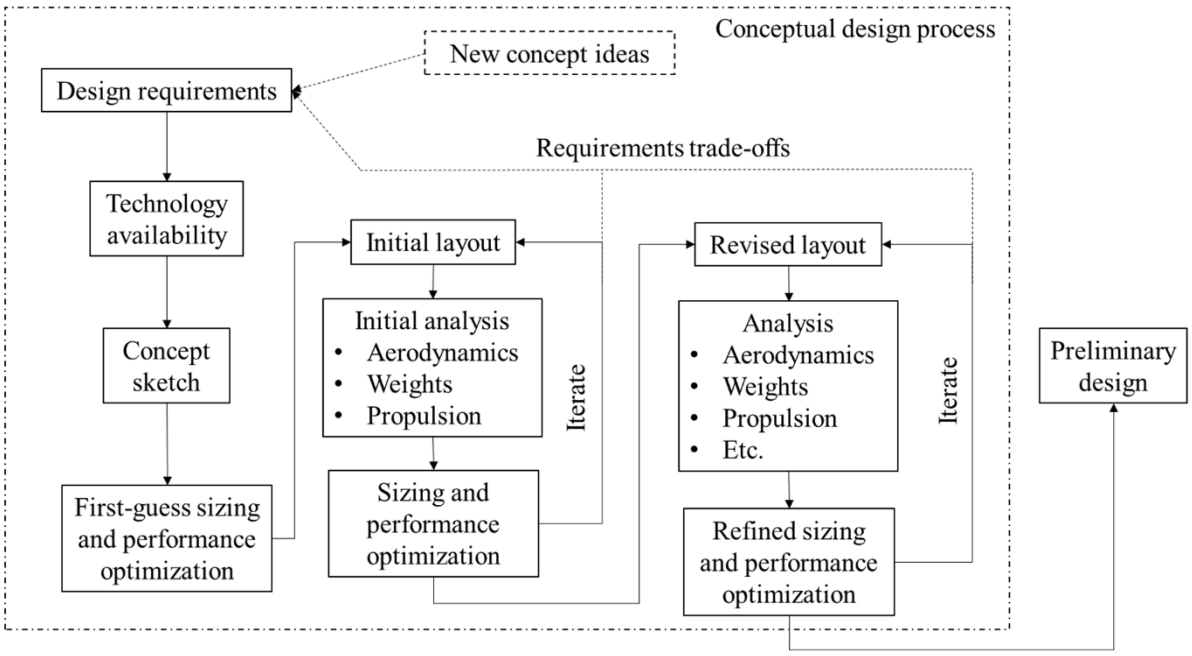

Figure SI 1. Conceptual aircraft design process (source [1])

The initial layout is examined to find out whether it will perform the mission as predicted by the first-order sizing. The actual weights, aerodynamics, and installed propulsion features are examined and are subsequently used for carrying out a detailed sizing calculation. Moreover, the performance capabilities of the design are estimated and compared to the mentioned requirements. Optimisation is used to find the lightest aircraft that will perform the design mission while meeting all performance requirements. The outcome of the optimisation comprises a better estimate of the necessary fuel weight and total weight for meeting the design mission. These also include necessary revisions to the wing and engine sizes. This often would require a fresh or revised design layout within which the designer implements these modifications and other changes recommended by other efforts. The revisions to the drawing, after some iterations, are then evaluated in detail by specialists, where they ensure that the design under consideration meets the requirements of their specialty. The final product of these efforts will be an aircraft design which can confidently be handed over to the next phase i.e., the preliminary design stage. Although further changes can be expected in the preliminary design phase, significant revisions will not take place if the efforts in the conceptual design phase have been successful.

SI 2. Aircraft data known and calculated

SI 2.1 Structural weight of different BWB aircraft sections

The three fuel cases that are examined are Jet-A, 100% synthetic paraffin kerosene (SPK) and liquid hydrogen (LH_2). Even though operating empty weight (OEW), payload weight, and gross take-off weight (GTOW) of N+2 blended wing body (BWB) powered by two ultra-high bypass ratio (UHB) geared turbofan engine (GTF) aircraft (301 passengers) is known from resource [4], the structural weight of different components or sections of the NASA N+2 BWB aircraft is required in the LH_2 aircraft design process primarily for restructuring the aircraft for the installation of LH_2 tank and insulation. NASA's study [4], which is used as a reference study for setting the design requirements for the current work, uses the 'Hybrid wing body Conceptual Design and structural optimisation' (HCDstruct) tool for modelling the BWB structure. The structural weights of different sections of NASA N+2 301 passenger BWB aircraft using HCDstruct is published in resource [5], which is summarised in Table SI 1. Resource [5] includes the structural analysis of the NASA N+2 301 passenger BWB aircraft which is based on a model validated with two separate BWB design cases. The structural addition to the BWB aircraft due to the LH_2 integral tank systems, comes in the form of a weight penalty. Verstraete [6] uses a weight penalty of 6% of the fuselage weight (of a tube-wing aircraft) to account for the additional structure required for attaching the structure of the integral LH_2 tank systems with the fuselage structure. In the current work, for the BWB aircraft the LH_2 tanks are installed in the inner wings and aft body. Therefore, the additional structural weight for installing the integral LH_2 tank systems is calculated to be 1,632 kg which is 6% of 27,220 kg (cumulative weight of the wings and aft body).

Table SI 1. Structural weights of different sections of NASA N+2 301 passenger BWB aircraft [5]

System	BWB aircraft section	Weight (kg)
1	Centre body	22,703
2	Cockpit	905
3	Aft body	4,074
4	Wing	23,146
5	Additional structural weight for installing integral LH_2 tank systems	1,633 [= 6% of 27,220 (3+4)]

SI 2.2 Structural weight of the conventional jet fuel and 100% SPK tank in BWB

The structural weight of the conventional jet fuel tank is important because this weight must be subtracted from the baseline BWB aircraft (powered by conventional jet fuel) and at the same time adding the LH_2 tank systems weight, while modelling the LH_2 aircraft. The structural weight of the conventional jet fuel tank in NASA N+2 301 passenger BWB aircraft is not known from any of NASA's studies [4,5,7–10]. Goraj [11] conducts design and optimisation of fuel tanks for BWB aircraft. Through their BWB aircraft design, Goraj finds that the weight of the conventional jet fuel tank systems is 284 tonnes (fuel weight and structural weight of tank) for fuel mass of 280 tonnes. Therefore, the structural weight of the conventional jet fuel tank is 4 tonnes for 280 tonnes of fuel mass. Referring to the reference study [4], the total fuel weight carried at mission start ($W_{F,total}$) (of conventional jet fuel) for NASA N+2 301 passenger BWB aircraft is known to be 73,965 kg. Therefore, for maintaining the same non-dimensional ratio of fuel weight and structural weight of tank of the study by Goraj, the structural weight of conventional jet fuel tank of the NASA N+2 301 passenger BWB aircraft is calculated to be 1,057 kg (~1.057 metric tonne).

Additionally, for 100% SPK there is a need for extra tank system. The additional tank weight will be estimated using the findings of the study by Goraj [11] discussed above. It will be observed in the result section (main paper) that this additional increase in tank weight for accommodating 100% SPK at mission start i.e., $W_{F,total}$ (slightly less mass dense), at start is insignificant (19 kg increase).

SI 2.3 LH_2 tank systems weight

A study by Khandelwal et al. [12] reviews different types of hydrogen tanks for aviation applications (configuration, shape, insulation, and tank materials). Another study by Verstraete et al. [13] examines different types of tank and insulation materials for hydrogen tanks for sub-sonic aviation application. Both studies suggest that integral type of hydrogen tanks of cylindrical shape with elliptical caps/heads are preferred for aviation applications. Aluminium alloy is the preferred tank wall material. An external tank insulation configuration using foam as the insulating material is preferable for the LH_2 tank to be used on a sub-sonic aircraft. These findings are used towards the selection of hydrogen tank type in this work.

The gravimetric index, gravimetric efficiency, or gravimetric storage density (η), which is defined as the ratio of cryogenic fuel weight to the sum of the dry tank weight and cryogenic fuel weight [13–16]. It is observed from our previous study [17] that foam-based cryogenic tanks for LH_2 aircraft with range greater than 9,000 km have $0.74 < \eta < 0.881$. The study by Beck et al. [18] models an LH_2 powered BWB very large twin aisle (VLTA) aircraft (design range 11,400 km for 531 passengers) that has tank $\eta = 0.77$. Advances in lighter and stronger composite materials have recently shown LH_2 cryogenic tank $\eta = 0.92$ for manufactured tanks [19] (which could improve in future), and that too for a small size tank (diameter 1.2 m and length 2.4 m). A study by Sjöberg et al. [20] model a light weight LH_2 tank (4.7 m length and 3 m diameter) using composite materials with $\eta = 0.94$ for a full tank, in comparison with metallic tank having $\eta = 0.71$. For LH_2 cases in this work, an average $\eta = 0.78$ with insulation thickness of 8.1 cm is used according to the study by Verstraete et al. [13] towards the estimation of the cryogenic tank systems weight for given $W_{F,total}$. Using $\eta = 0.78$ for a given (capacity) $W_{F,total}$, the unknown i.e., tank weight, can be estimated.

SI 2.4 BWB aircraft geometry

SI 2.4.1 Selection of BWB airfoils

In terms of aircraft geometry, the data for NASA N+2 BWB aircraft is not completely known from the (NASA) study by Nickol et al. [4] (used as a reference study for setting design requirements in the current work). One of the designers/authors of NASA's BWB known from resource [4], was associated with Garmendia's PhD thesis [21], where the air-foil thickness to chord ratio (t/c) of the BWB 301 is indicated.

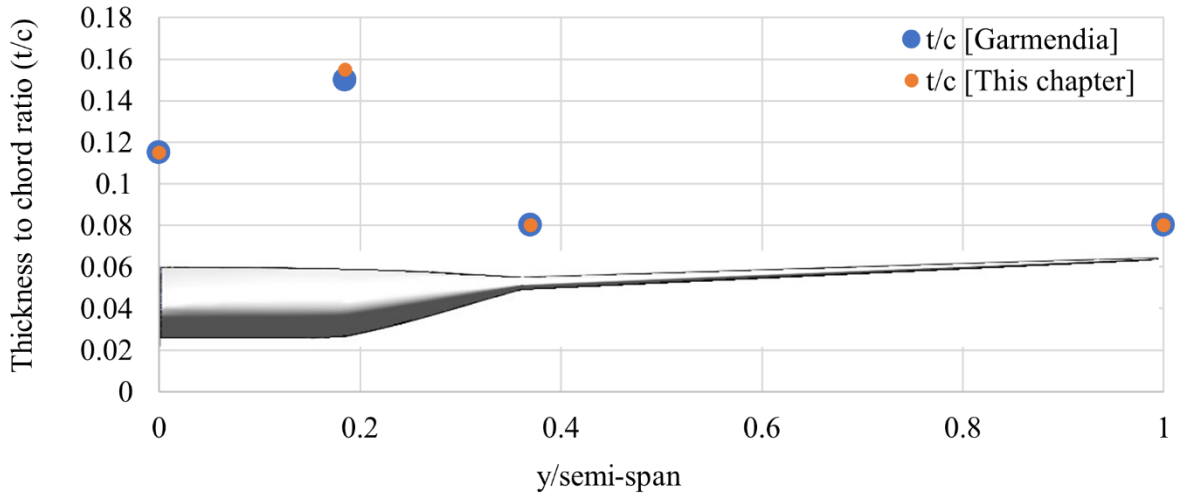

Figure SI 2. Thickness to chord (t/c) ratio of the transonic air-foils along the span for BWB geometric modelling (using data from [21])

The t/c ratio of the transonic airfoils used for BWB geometric modelling in this work is provided in Figure SI 2. Figure SI 2 shows the comparison of the t/c from the study by Garmendia and t/c used in this work. At the aircraft root 11.5% t/c is recommended by Garmendia and the same t/c is used here (air-foil coordinates source [22]). At the end of cabin (y/semi-span of 18%), 15% t/c is recommended by Garmendia and 15.5% t/c is used here as this is the closest available transonic air-foil in open literature (air-foil coordinates source [23]).

For outer wings 8% t/c is recommended by Garmendia and the same t/c is used here (air-foil coordinates source [24]).

SI 2.4.2 Other geometric dimensions

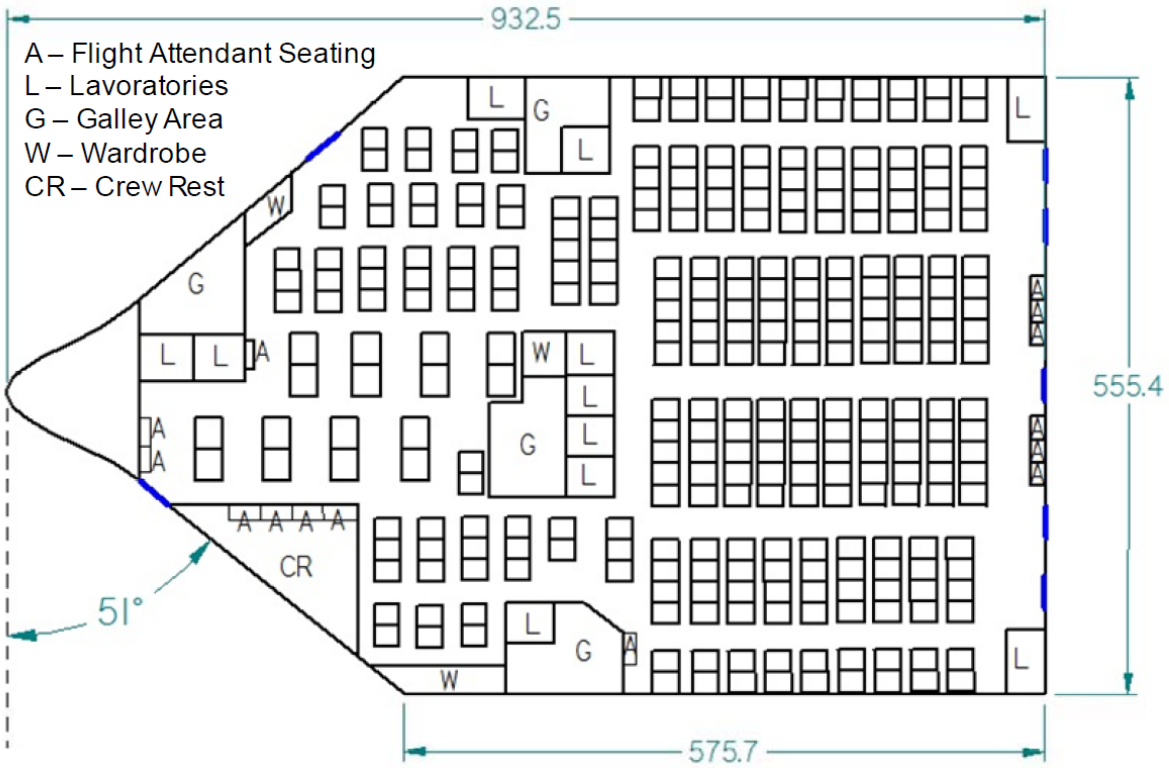

Figure SI 3. Cabin layout of NASA N+2 BWB aircraft for 301 passengers where dimensions are in inches (source [10], Copyright: work of the US government and public use is permitted)

In terms of the geometric dimensions, except the span no other dimension are known for the NASA N+2 BWB aircraft from resources [4,5,7–10]. The span of the aircraft under design consideration is known to be 76.2 m. A study by June et al. [25] indicates three-view engineering drawings of the NASA N+2 BWB aircraft that seats 301 passengers. Knowing the aircraft span, the other geometric information of the aircraft will be estimated via a reverse engineering approach. Using the three-view engineering drawing, the outer mould line of the aircraft will be developed in SolidWorks. Figure 1 in resource [25] shows the three-views of NASA N+2 BWB aircraft for 301 passengers. From the top view of this figure, the aircraft outer mould line (OML) can be traced in SolidWorks by setting the aircraft span to 76.2 m. Once the OML is traced with the known span as a reference, the remaining geometric information can be obtained. The wing dihedral angle is also estimated using SolidWorks from the front view. Based on the front and top view of the aircraft, the airfoils are positioned along the spanwise direction (known from SI § 2.4.1). Figure SI 3 shows the cabin layout of NASA N+2 BWB aircraft for 301 passengers. It is to be noted that the dimensions in the said figure are in inches. The length of the cabin is 23.67 m, and the maximum cabin width is 14.11 m.

SI 3. Aircraft weight sizing methodology

SI 3.1 Propulsion

The propulsion aspect of the weight sizing process is described in detail in [26]. UHB GTF engines are designed for the set research objectives and design requirements, which powers the BWB aircraft using conventional jet fuel, 100% SPK, and LH_2 fuel (separately). The results for engines fired by conventional jet fuel, 100% SPK, and LH_2 fuel comprise of performance analysis at on-design point and all off-design points, along with the engine weight. The thrust specific fuel consumption (TSFC) at all points in the flight mission profile (discussed in main paper §2.3) are input to the weight sizing process. More specifically, they are inputs to Breguet's range equation (discussed ahead in detail) which is used for estimating the fuel mass consumed during the aircraft operation. Additionally, the engine weights are inputs to the aircraft weight sizing process, as these contribute to GTOW of the aircraft which determines the fuel consumed over the flight mission.

SI 3.2 Aerodynamics

In terms of aerodynamics, the lift to drag ratio (*L/D*) is calculated using standard equations at three operating conditions: climb, cruise, and loiter. The drag coefficient (C_{D}) is estimated using equation SI 1, assuming that it is the sum of the zero-lift drag coefficient and lift-induced drag coefficient, and that there is no wave drag,

$$C_{\mathrm{D}} = C_{\mathrm{D},0} + \frac{C_{\mathrm{L}}^2}{\pi\,\mathrm{AR}\,\mathrm{e}}, \tag{SI 1}$$

$$\text{where } C_{\mathrm{D},0} = \frac{C_{\mathrm{f}}\ S_{\mathrm{wet}}}{S}, \text{ and} \tag{SI 2}$$

$$C_{\mathrm{L}} = \frac{W_{\mathrm{aircraft}}}{0.5\ \rho_{\mathrm{a}}\ S\ V^2}\ . \tag{SI 3}$$

$C_{\mathrm{D},0}$ is the coefficient of zero-lift drag, C_{L} is the coefficient of lift, AR is the aspect ratio for a given aircraft, and *e* is the Oswald's efficiency factor – a correction factor that is representative of change in drag with lift of a 3D wing in comparison with an ideal wing that has same AR with an elliptical lift distribution. Wave drag modelling is a high order or high-fidelity analysis, which is beyond the scope of this work. AR, e, and C_{f} are respectively known to be 6.1 (Table 1 in main paper), 0.85 (for large twin aisle [LTA] aircraft [27]), and 0.0025 (modern/advanced large transport jets [28]). The aircraft wetted area (S_{wet}), is estimated from the aircraft geometric model developed in SolidWorks. The wing area (*S*) is known from Table 1 in the main paper to be 944.73 m^2 for the NASA N+2 BWB aircraft. GTOW can be calculated once the weights of all aircraft systems are known. The lift coefficient is given by equation SI 3. Knowing the Mach number and altitude for climb, cruise, and loiter, both airspeed (V) and air density (ρ_a) are known. The aircraft weight (W_{aircraft}) at climb, cruise, and loiter, is the average weight (of start and end of each operation) of the aircraft during each of the three conditions, estimated from the weight sizing process. After both the lift coefficient and drag coefficient are

calculated, *L/D* is calculated for the climb, cruise, and loiter. In cruise, the aircraft thrust to weight ratio (*T/W*) is equal to the reciprocal of the *L/D* ratio of the aircraft. The (minimum) thrust requirement at cruise is calculated from the estimated *L/D* and aircraft weight, as both are known from the weight sizing process.

SI 3.3 Fuel fraction for Jet-A, SPK and LH_2

The fuel fraction (FF) is a measure of the fuel consumed during a given aircraft operation. For example: FF value of 0.995 for taxi-out operation means that the weight of fuel consumed during taxi-out operation is (1-0.995 =) 0.5% of the aircraft weight at the beginning of taxi-out operation. FF can be used for individual aircraft mission segments such as taxi, cruise, descent, etc. and/or for the entire mission. The product of FFs for all mission segments represents the FF of the aircraft over the entire mission. For example: If the product of all FFs is 0.8 then it means that the weight of fuel consumed during entire mission is (1-0.8 =) 20% of the aircraft weight at the beginning of the mission.

Table SI 2. Fuel fraction provided by Roskam [2] with recommended modifications to Roskam's FFs for Jet-A, and FFs recommended for LH_2

Segment	Operation	Roskam's FFs (Jet-A) [2]	Modified FFs (Jet-A)	FFs (LH_2)
1	Engine start and warmup	0.99	0.9964	0.9987
2	Taxi-out	0.99	0.9964	0.9987
3	Take-off	0.995	0.9982	0.9994
4	Climb	0.98	$M_{ff,climb}$	$M_{ff,climb}$
5	Cruise	$M_{ff,cruise}$	$M_{ff,cruise}$	$M_{ff,cruise}$
6	Descent	0.99	0.9964	0.9987
7	Loiter	$M_{ff,loiter}$	$M_{ff,loiter}$	$M_{ff,loiter}$
8	Land, taxi-in, engine shutdown	0.992	0.9971	0.9989
	Overall FF	Product (1-8)	Product (1-8)	Product (1-8)

Table SI 3. Fuel fraction (FF) provided by Roskam [2] with recommended modifications to Roskam's FFs for Jet-A, and FFs recommended for 100% SPK

Segment	Operation	Modified FFs (Jet-A)	FFs (100%SPK)
1	Engine start and warmup	0.9964	0.9965
2	Taxi-out	0.9964	0.9965
3	Take-off	0.9982	0.9982
4	Climb	$M_{ff,climb}$	$M_{ff,climb}$
5	Cruise	$M_{ff,cruise}$	$M_{ff,cruise}$
6	Descent	0.9964	0.9965
7	Loiter	$M_{ff,loiter}$	$M_{ff,loiter}$
8	Land, taxi-in, engine shutdown	0.9971	0.9972
	Overall FF	Product (1-8)	Product (1-8)

Roskam [2] provides the FFs for a transport jet using conventional jet fuel (Jet-A). Roskam's FFs for all mission segments except cruise and loiter, are provided in Table SI 2. For a long-range LTA aircraft that is considered in this work, the fuel expenditure in non-cruise and non-loiter phases is significantly lower as compared to that in cruise and loiter phases. The product of these FFs (not including cruise and loiter FFs) by Roskam is approximately 0.936, which means that weight of fuel consumed in these mission segments is 6.143% of GTOW of the aircraft. For cruise and loiter, the FFs can be calculated using Breguet's range equation (discussed ahead).

The FF for climb, cruise, and loiter can be calculated using equations SI 4, SI 5, and SI 6 respectively (discussed next). However, Roskam's FFs are based on historical data (older aircraft before 1990s). The fuel efficiency of aircraft introduced in the past two decades have improved significantly. Therefore, there is a need for modifying the FFs provided by Roskam, based on the recent literature. The GBD report of the Royal Aeronautical Society [29] and the study by Kenway et al. [30], both model the aircraft performance using the modified Breguet's range equation. For all operations except cruise and loiter, both studies model the weight of fuel consumed to be 2.2% of GTOW (also used for modelling in our previous studies [17,31]). This weight of fuel consumed (2.2% of GTOW) during all operations except cruise and loiter is 64.19% less than the fuel weight predicted using Roskam's FF (6.143%). As mentioned before, the Roskam's FF are based on historical aircraft and thus modifications are recommended. The modified FF (64.19% improvement to Roskam's FF) for Jet-A are listed in Table SI 2. For example: FF value of 0.99 for taxi-out operation means that the weight of fuel consumed during taxi-out operation is (1-0.99 =) 1% of the aircraft weight at the beginning of taxi-out operation. The improvement of 64.19% means that instead of 1% GTOW, only 35.81% of 1% GTOW was the amount of fuel consumed. Therefore, the FF is 0.9964. It is to be noted that for the 'climb' operation, Roskam provides a defined value of FF for historical aircraft. In this work, modifications are not made to the defined value by Roskam (FF) for climb phase as the performance during the climb operation will be modelled using Breguet's range equation as represented by equation SI 4 (discussed next). The reason for this is that compared to the other operations except cruise and loiter, the effects of better aircraft aerodynamics of a BWB is prominently observed during climb.

If the GTOW is 300,000 kg for a Jet-A aircraft and the modified Roskam's FF for 'engine start and warmup' operation is 0.9964 (from Table SI 2), then the fuel consumed during this aircraft operation is [300,000 x (1-0.9964) =] 1,080 kg and the aircraft weight at the end of this operation or in the beginning of (the next operation) take-off is [300,000 – 1,080 =] 298,920 kg. Similarly, for each of the other mission segments the aircraft weight and fuel consumption for respective mission segments, are calculated. $W_{F,block}$ is the block fuel weight which is defined as the total fuel weight consumed in all segments in the mission.

For LH_2 powered BWB aircraft, the FFs are different compared to Jet-A case. This is because for same work output if 1 kg of LH_2 fuel is used, then 2.865 kg of Jet-A is consumed equivalently (as studied in [17,31] and [26]). Therefore, this results in weight reduction of 65.1% and lower fuel mass of LH_2 need to be carried on the aircraft. This effect is reflected through the FFs as shown in Table SI 2. The FF calculation for LH_2 is as follows. For example: The modified FF for Jet-A during the taxi-out operation is 0.9964, which means that the fuel weight consumed during the taxi-out operation is 0.36% of aircraft weight at the start of the

taxi-out stage. For the same energy content during the taxi-out stage, accounting the 65.1% reduction in fuel weight (described above) while switching from Jet-A to LH_2, the FF for LH_2 is calculated to be [0.9964 + (1-0.9964) x (1-(1/2.865)) =] 0.9987 i.e., LH_2 fuel weight is 0.13% of aircraft weight at the start of the taxi-out stage. Similarly, the other FFs are calculated and listed in Table SI 2 for LH_2 powered aircraft. This is similar to the approach used by Beck et al. [18] for their LH_2 powered VLTA BWB aircraft.

The FFs of 100% SPK powered aircraft are expected to be slightly different than the FFs of Jet-A aircraft since SPKs have slightly higher gravimetric energy density than Jet-A. Recalling the results of engine performance from [26], for the same thrust production, the energy released by 1 kg Jet-A is equal to energy released by 0.98 kg of 100% SPK (2% fuel weight saving). This effect is reflected through the FFs as shown in Table SI 3. The FF calculation for different SPKs is as follows. For example: The modified FF for Jet-A during the taxi-out operation is 0.9964, which means that the fuel weight consumed during the taxi-out operation is 0.36% of aircraft weight at the start of the taxi-out stage. For the same energy content during the taxi-out stage, accounting 2% reduction in fuel weight (described above) while switching from Jet-A to 100% SPK, the FF for 100% SPK is calculated to be [0.9964 + (1-0.9964) x (1-0.98) =] 0.9965. Similarly, the other FFs are calculated and listed in Table SI 3 for different SPK powered aircraft.

For each of the mission segments, the FF determines the fuel consumed during that mission segment for known aircraft weight at the beginning of that mission segment. Therefore, using FF the aircraft weight at end of a mission segment or beginning of the next mission segment can be calculated, for a known mission profile. The FF during climb ($M_{ff,climb}$) is calculated from Breguet range equation with the form seen in equation SI 4, and is given by,

$$M_{ff,climb} = \frac{1}{e^{\left[\left(\frac{endurance}{60}\right)*TSFC \Big/ \left(\frac{L}{D}\right)\right]}}, \quad \text{(SI 4)}$$

where endurance during climb is calculated in minutes [and equals the ratio of cruise altitude and rate of climb (RoC)]. The RoC used is 3,000 ft/min [32] or 914.4 m/min (standard value used for transport jets) to a cruise altitude of 10,668 m (or 35,000 ft in the current work as per design requirements or mission profile discussed in §2.3 of the main paper). For the cruise and loiter (additional cruise), the method is similar. Instead of using endurance in the equation, both range and velocity are input (values are known from §2.3 of the main paper). The FF during cruise ($M_{ff,cruise}$) is calculated from Breguet range equation with the form seen in equation SI 5, and is given by,

$$M_{ff,cruise} = \frac{1}{e^{\left[cruise\ range*TSFC \Big/ V*\left(\frac{L}{D}\right)\right]}}, \quad \text{(SI 5)}$$

and the FF during loiter ($M_{ff,loiter}$) is calculated from Breguet range equation with the form seen in equation SI 6, and is given by,

$$M_{ff,loiter} = \frac{1}{e^{\left[loiter\ range*TSFC \Big/ velocity*\left(\frac{L}{D}\right)\right]}}. \quad \text{(SI 6)}$$

The product of all FFs in the mission gives the FF value for the entire mission. The TSFC values for climb, cruise, and loiter come from the engine model developed in GasTurb 13 software tool [33] (see [26]), and *L/D* calculation as described in SI §3.2.

The average aircraft weight during climb, cruise, or loiter, is absorbed in equations SI 1 – SI 3 that enable the estimation of *L/D*. After GTOW is estimated, using the above FFs, the aircraft weight at beginning of climb can be calculated but the aircraft weight at the end of climb is unknown and so is the *L/D*. Both *L/D* and aircraft weight at the end of climb are calculated through simple iteration looping, as they are linked via weight sizing process. Similar approach is used for cruise and loiter for the estimation of *L/D* and aircraft weight at the end, of respective aircraft operation.

SI 3.4 Aircraft systems weight

In the current work, three separate BWBs are considered for design analysis. The first is powered by conventional jet fuel (Jet-A), the second is powered by LH_2 and the third is powered by 100% SPK fuel. Table SI 4 lists the aircraft systems weight for Jet-A BWB aircraft (baseline) and LH_2 BWB aircraft. Similarly, Table SI 5 lists the aircraft systems weight for Jet-A BWB aircraft (baseline) and 100% SPK BWB aircraft.

SI 3.4.1 Jet-A BWB aircraft

As discussed in §7.3, the ratio of $W_{F,block}$ and $W_{F,total}$ of the Jet-A NASA N+2 BWB aircraft is 0.9 [4]. In this work, similar value for the said ratio is used during the iteration process of the weight sizing process for estimating the aircraft operational energy consumption. For the BWB conventional jet fuel (baseline) case of this work, except for the engine weights and $W_{F,total}$, there is no other change compared to the Jet-A BWB aircraft [4].

The total propulsion systems weight comprises of weight of the bare engine, nacelle, inlet, mounting, and accessories, for two engines. GTOW of Jet-A BWB aircraft is essentially OEW from the Nickol et al. [4] study minus the total propulsion systems weights predicted by Nickol et al., and adding the total propulsion systems weights estimated from [26], the design payload weight and $W_{F,total}$ (calculated iteratively) as indicated in Table SI 4. Therefore, for Jet-A BWB aircraft, beginning with a guess of $W_{F,total}$, all inputs are known for estimating the mission fuel burn. Knowing GTOW, the aerodynamics (SI §3.2), the FFs (modified FFs and FFs based on Breguet's range equation for Jet-A, from SI §3.3), and TSFCs at different points in flight mission ([26]), $W_{F,block}$ for Jet-A BWB aircraft can be calculated iteratively according to the flowchart shown in Figure 2 (main paper) until the ratio of $W_{F,block}$ and $W_{F,total}$ of 0.9 is met.

SI 3.4.2 LH_2 BWB aircraft

The weight sizing process that calculates the mission/block fuel consumption, is more iterative for LH_2 BWB aircraft as compared to Jet-A BWB aircraft. This is because LH_2 BWB aircraft has addition of new components like the LH_2 tank systems and additional structural weight for installing the integral LH_2 tank systems, along with the LH_2 fired propulsion systems.

Table SI 4. Aircraft systems weight for Jet-A BWB aircraft (baseline) and LH_2 BWB aircraft

System	Aircraft system	Weight (kg)	Source
1	Total propulsion systems weight [2 x (weight of bare engine + nacelle + inlet + mounting + accessories)]	17,076	[4]
2	OEW (NASA BWB)	114,907	[4]
3	Weight of the conventional jet fuel tank	1,057	Calculated in SI §2.2
4	OEW without propulsion systems and tank	96,774	= 2-1-3
5	Payload weight (design)	53,570	[4]
6	$W_{F,total}$ (Jet-A)		Calculated iteratively using ratio of 0.9 of $W_{F,block}$ and $W_{F,total}$
7	GTOW of NASA N+2 BWB (301 passengers) Jet-A aircraft	242,441	[4] or (2+5+6)
8	Total propulsion systems weight in the present work [2 x (weight of bare engine + nacelle + inlet + mounting + accessories)]		Based on [26] (Jet-A and/or LH_2 engines)
9	GTOW of Jet-A BWB aircraft (baseline) [current work]		= 2-1+8+5+6
10	Weight of LH_2 tank systems		Calculated using model described in SI §2.3
11	Additional structural weight for installing integral LH_2 tank systems	1,633	Calculated in SI §2.1
12	$W_{F,total}$ for LH_2 BWB aircraft		Calculated iteratively using ratio of 0.9 of $W_{F,block}$ and $W_{F,total}$
13	GTOW of LH_2 BWB aircraft [current work]		= 4+8+5+10+11+12

The hydrogen fuel systems for an aircraft comprise of storage tanks, a feed and distribution system, and an interface fuel panel [34]. The feed and distribution system consists of all lines, valves, pressure and temperature sensors, heat exchangers, pumps, and regulators needed to create a safe cryogenic fuel system. As discussed in [26], considering that hydrogen has higher flame speeds as compared to Jet-A fuel, the diameter of the hydrogen fuel lines is expected to be lower than that for Jet-A. This has a potential to reduce the weight of fuel lines. The effect of above-mentioned hydrogen fuel systems except the fuel storage tank, on aircraft weight is assumed to be negligible in this work.

Table SI 5. Aircraft systems weight for Jet-A BWB aircraft (baseline) and 100% SPK BWB aircraft

System	Aircraft system	Weight (kg)	Source
1	Total propulsion systems weight [2 x (weight of bare engine + nacelle + inlet + mounting + accessories)]	17,076	[4]
2	OEW (NASA BWB)	114,907	[4]
3	Weight of the conventional jet fuel tank	1,057	Calculated in SI §2.2
4	OEW without propulsion systems and tank	96,774	= 2-1-3
5	Payload weight (design)	53,570	[4]
6	$W_{F,total}$ (Jet-A, NASA)	73,965	[4]
7	$W_{F,total}$ (calculated in this work)	Calculated iteratively using ratio of 0.9 of $W_{F,block}$ and $W_{F,total}$	
8	GTOW of NASA N+2 BWB (301 passengers) Jet-A aircraft	242,441	[4] or (2+5+6)
9	Total propulsion systems weight in present work [2 x (weight of bare engine + nacelle + inlet + mounting + accessories)]	Based on [26] (Jet-A and/or SPK engines)	
10	GTOW of Jet-A BWB aircraft (baseline) [current work]		= 2-1+9+5+7
11	Additional weight of 100% SPK tank systems	Calculation described in SI §2.2	
12	$W_{F,total}$ for SPK BWB aircraft	Calculated iteratively using ratio of 0.9 of $W_{F,block}$ and $W_{F,total}$	
13	GTOW for 100% SPK BWB aircraft [current work]		= 2-1+9+5+11+12

GTOW of the LH_2 powered aircraft will be different than that of the conventional jet fuel powered aircraft because of lower weight of hydrogen fuel to be carried on-board, addition of LH_2 tank systems, and additional structural weight for installing the integral LH_2 tank systems in the BWB aircraft, along with the LH_2 fired propulsion systems. As shown in Table SI 4, GTOW of LH_2 BWB aircraft is calculated by: subtracting the total weight of Jet-A propulsion system (17,076 kg) [Nickol et al. [4] study] and the weight of conventional jet fuel tank (1,057 kg) from the OEW of NASA N+2 BWB (301 passengers) Jet-A aircraft (of 114,907 kg), and then adding: the total LH_2 fired propulsion systems weight (based on [26]), the payload weight (53,570 kg), the weight of LH_2 tank systems (calculation described in SI §2.3), the additional structural weight for installing the integral LH_2 tank systems (1,633 kg, calculated in SI §2.1), and $W_{F,total}$ (calculated iteratively for maintaining the same ratio of $W_{F,block}$ and $W_{F,total}$, as that for Jet-A BWB aircraft, of 0.9). The iterative process for LH_2 BWB aircraft is discussed in detail in §2.5 (main paper).

SI 3.4.3 SPK BWB aircraft

100% SPK case requires insignificant modification to tank system as the density of 100% SPK is slightly lower than Jet-A as discussed in [26] and in SI §2.2. GTOW of 100% SPK powered aircraft will be different than that of the conventional jet fuel powered aircraft because of slightly lower fuel weight of 100% SPK fuel (as this fuel has slightly high gravimetric energy density) to be carried on-board compared to Jet-A case. As shown in Table SI 5, GTOW of 100% SPK BWB aircraft is calculated by: subtracting the total weight of Jet-A propulsion system (17,076 kg) [Nickol et al. [4] study] from the OEW of NASA N+2 BWB (301 passengers) Jet-A aircraft (of 114,907 kg), and then adding: the total SPK powered propulsion systems weight (based on [26]), the payload weight (53,570 kg), and $W_{F,total}$ of 100% SPK carried on the aircraft (calculated iteratively for maintaining the same ratio of $W_{F,block}$ and $W_{F,total}$, as that for Jet-A BWB aircraft, of 0.9). Additionally, for the 100% SPK case there is an (insignificant) addition of extra tank system for accommodating a slightly less dense fuel than Jet-A. The iterative process for 100% SPK BWB aircraft is discussed in detail in §2.5 (main paper).

SI 4. Results

SI 4.1 Iteration parameters for LH_2 aircraft cases

Table SI 6. Convergence criteria and T/W ratio constraints for LH_2 aircraft cases during the iteration of the weight sizing process

Parameter	Value
Convergence criteria* (Ratio of $W_{F,block}$ and $W_{F,total}$)	0.9
Minimum *T/W* at top of climb (TOC)**	0.04851
Minimum *T/W* at sea level static (SLS)**	0.262

* For all three cases of LH_2 aircraft

** Only for case 2 and 3 of LH_2 aircraft (as described in section 7.4.5)

For the Jet-A BWB aircraft case, using the weight sizing process, the ratio of $W_{F,block}$ and $W_{F,total}$ is 0.9. For 100% SPK and three cases of LH_2 considered in this work, the above ratio of $W_{F,block}$ and $W_{F,total}$ (of 0.9) is set as the convergence criteria for the weight sizing process, according to the methodology described in §2.5 (main paper).

Additionally, using the weight sizing process for the Jet-A BWB aircraft and known data, the *T/W* ratios at sea level static (SLS) and top of climb (TOC) are calculated to be 0.262 and 0.04851, respectively. These two *T/W* ratios are set as constraints (minimum values to be met) in the weight sizing process for both Cases 2 and 3 of LH_2 aircraft, according to the methodology described in §2.5 (main paper). Case 1 of LH_2 aircraft, by the problem formulation, remains unaffected by the lighter aircraft (LH_2 use) and its engines produce the same thrust as produced by the engines of Jet-A BWB aircraft. Similarly, 100% SPK BWB aircraft remains unaffected by the slightly lighter aircraft and their engines produce the same thrust as produced by the engines of Jet-A BWB aircraft. Therefore, the *T/W* ratio (minimum)

constraints at SLS and TOC (0.262 and 0.04851 respectively) are not considered for iteration purposes in the weight sizing process for case 1 of LH_2 aircraft and 100% SPK. Resultantly, *T/W* at SLS and TOC for case 1 of LH_2 aircraft is greater than Jet-A BWB aircraft, and case 2 and 3 of LH_2 aircraft, because it is an unoptimized case where the engines are producing more thrust than required, for a lighter aircraft. Similarly, *T/W* at SLS and TOC for 100% SPK aircraft is slightly greater than Jet-A BWB aircraft. The convergence criteria and *T/W* constraints are summarised in Table SI 6.

SI 4.2 Aerodynamics

The BWB wingspan, *S*, and AR in this work (for Jet-A use, 100% SPK use, and LH_2 use [all three cases]) are 76.2 m, 944.73 m^2, and 6.1, respectively, as discussed in section 7.3.1. S_{wet} (for Jet-A use, 100% SPK use, and LH_2 use [all three cases]) is calculated to be 2,132 m^2 (22,944 ft^2) using the SolidWorks geometric model.

The cruise *L/D* ratio of the NASA N+2 BWB aircraft (Jet-A) is 23.7 [4]. In this work, through the weight sizing process of the BWB the cruise *L/D* ratio for Jet-A, Case 1 LH_2, Case 2 LH_2, Case 3 LH_2, and 100% SPK are 23.7, 22.51, 22.45, 22.36, and 23.66, respectively. It can be observed that the cruise *L/D* ratio of the Jet-A and 100% SPK BWB case are similar to values for the NASA N+2 BWB aircraft (Jet-A).

SI 4.3 Propulsion

SI 4.3.1 TOC thrust prediction

As discussed previously, the required thrust at the TOC point is predicted by two methods. The first method is using the service ceiling thrust equation, and the second method is using the *T/W* ratio of the baseline (Jet-A BWB aircraft) case. The inputs to the service ceiling equation come from the weight sizing process and the *T/W* ratio at TOC for the (baseline) Jet-A BWB aircraft is calculated to be 0.04851 (as discussed before). The aircraft weight at the end of climb is known from the weight sizing process and using the known *T/W* ratio of 0.04851, the required thrust can be calculated. The maximum of thrust values calculated using the above two methods becomes the thrust required to be produced.

Table SI 7. Prediction of TOC thrust using the service ceiling equation and the constraint of T/W ratio of 0.04851 for LH_2 aircraft cases

TOC thrust prediction (per engine) using:	Jet-A (kN)	LH_2 (kN)		
		Case 1	Case 2	Case 3
1. Service ceiling equation (section 7.3.3)	54.83	46.17	45.94	45.63
2. *T/W* ratio of 0.04851	*	46.29	46.02	45.66
Thrust produced ([26])	55.603	55.603**	46.35	46.12

*For Jet-A case, the thrust at TOC is known to be 55.603 kN as per the design requirements set by using Nickol et al. [4] study

** Case 1 is where thrust production remains unchanged (not optimised)

Table SI 8. Prediction of TOC thrust using the service ceiling equation and the constraint of T/W ratio of 0.04851 for 100% SPK aircraft

TOC thrust prediction (per engine) using:	Jet-A (kN)	100% SPK
1. Service ceiling equation (section 7.3.3)	54.83	54.46
2. *T/W* ratio of 0.04851	*	55.24
Thrust produced ([26])	55.603	55.603

*For Jet-A case, the thrust at TOC is known to be 55.603 kN as per the design requirements set by using Nickol et al. [4] study

The comparison of thrust prediction at TOC using the two methods is summarised in Table SI 7 and Table SI 8 for LH_2 and 100% SPK, respectively, relative to the baseline Jet-A case. It is to be noted that the thrust per engine is known to be 55.603 kN, which is a design requirement. Hence this thrust value determines the *T/W* ratio at the TOC point. Thus, this thrust value is not listed corresponding to the second method that uses the TOC *T/W* ratio of 0.04851, and the above discussion is noted in Table SI 7 and Table SI 8. Additionally, LH_2 Case 1 is where thrust production remains unchanged, by problem definition, despite the thrust requirement being lower since the aircraft is lighter due to use of LH_2 fuel (high gravimetric energy density).

As can be observed from Table SI 7 and Table SI 8, the required thrust predicted by using both the service ceiling equation and the *T/W* ratio, are very similar. This builds a confidence in the model developed. Additionally, the thrust per engine at TOC is known to be 55.603 kN from the design requirement based on Nickol et al. [4] study, for Jet-A case. The service ceiling equation, which takes inputs from the weight sizing process discussed in this work predicts thrust per engine of 54.83 kN. It is to be noted that this difference is because the Jet-A engines used in Jet-A BWB aircraft are significantly lighter than engines used in Nickol et al. [4] study and $W_{F,total}$ is calculated to be lower than Nickol et al. study (see [26]). The total propulsion systems weight comprises of the weight of bare engine, nacelle, inlet, mounting, and accessories, for two engines. The total propulsion systems weight of Nickol et al. [4] study and the Jet-A BWB aircraft in this work (see [26] for details) are 17,076 kg and 12,319 kg, respectively. The Jet-A BWB aircraft designed in this work is lighter than NASA N+2 BWB aircraft by Nickol et al. [4], which results in a lower thrust requirement. Therefore, this difference in the thrust is anticipated. Despite this non-uniformity, the thrust prediction between the two methods is similar. As LH_2 aircraft gets more optimised (case 2 and 3), the thrust requirement reduces as compared to case 1, which is anticipated.

SI 4.3.2 Propulsion systems performance and weight

The inputs (performance parameters) to the weight sizing process for Jet-A and the three cases of LH_2 are summarised in Table SI 9, and for Jet-A and 100% SPK are summarised in Table SI 10. These are selected parameters that are relevant to the weight sizing process. The reader is advised to see [26] to find other parameters related to the propulsion systems (not relevant to the discussion in this work). The total propulsion systems weight of Nickol et al. [4] study is 17,076 kg. It can be observed from Table SI 9 that the total propulsion systems weight of Nickol et al. study is significantly greater than Jet-A case (and 100% SPK) of the

current work (by ~4.7 tonnes) and all three cases of LH_2 (by ~4.8 tonnes, ~5.4 tonnes and ~6.3 tonnes for case 1, 2, and 3, respectively). The discussion on the reasons for the propulsion systems weight reduction is detailed in [26]. Additionally, it can be observed from Table SI 10 for 100% SPK case the total propulsion systems weight is similar to the for Jet-A case of this work.

Table SI 9. Performance of propulsion system at different points in the flight mission profile for Jet-A and LH_2 fuel (three cases) and their weights

Parameters		Units	Jet-A	LH_2		
				Case 1	Case 2	Case 3
Total propulsion systems weight		kg	12,319	12,259	11,666	10,769
Performance characteristics per engine						
TOC	Mach, altitude	- , m	0.8 at 10,668 m	0.8 at 10,668 m	0.8 at 10,668 m	0.8 at 10,668 m
	TSFC	g/kN-s	12.400	4.328	4.284	4.160
	Thrust required	kN	55.603	46.29	46.02	45.66
	Thrust produced	kN	55.603	55.603	46.354	46.12
Cruise	Mach, altitude	- , m	0.84 at 10,668 m	0.84 at 10,668 m	0.84 at 10,668 m	0.84 at 10,668 m
	TSFC	g/kN-s	12.667	4.424	4.351	4.278
	Thrust required	kN	42.25	40.24	40.15	40.02
	Thrust produced	kN	51.61	51.68	51.09	43.12
SLS	Mach, altitude	- , m	0 at 0 m	0 at 0 m	0 at 0 m	0 at 0 m
	TSFC	g/kN-s	5.124	1.778	1.761	1.690
	Thrust required	kN	299.9	251.09	249.62	247.69
	Thrust produced	kN	303.89	304.53	263.83	261.14
Climb	Mach, altitude	- , m	0.47 at 5,334 m	0.47 at 5,334 m	0.47 at 5,334 m	0.47 at 5,334 m
	TSFC	g/kN-s	9.798	3.413	3.389	3.266
	Thrust produced	kN	94.94	95.54	96.96	82.58
Loiter	Mach, altitude	- , m	0.6 at 1,500 m	0.6 at 1,500 m	0.6 at 1,500 m	0.6 at 1,500 m
	TSFC	g/kN-s	12.175	4.234	4.195	4.067
	Thrust produced	kN	114.67	115.46	120.05	98.02

Table SI 10. Performance of propulsion system at different points in the flight mission profile for Jet-A and SPKs and their and weights

Parameters		Units	Jet-A	100% SPK
Total propulsion systems weight		kg	12,319	12,319
Performance characteristics per engine				
TOC	Mach, altitude	- , m	0.8 at 10,668 m	0.8 at 10,668 m
	TSFC	g/kN-s	12.400	12.150
	Thrust required	kN	55.603	55.24
	Thrust produced	kN	55.603	55.603
Cruise	Mach, altitude	- , m	0.84 at 10,668 m	0.84 at 10,668 m
	TSFC	g/kN-s	12.667	12.411
	Thrust required	kN	42.25	42.16
	Thrust produced	51.61kN	51.61kN	51.61kN
SLS	Mach, altitude	- , m	0 at 0 m	0 at 0 m
	TSFC	g/kN-s	5.124	5.022
	Thrust required	kN	299.9	301.83
	Thrust produced	kN	303.89	303.85
Climb	Mach, altitude	- , m	0.47 at 5,334 m	0.47 at 5,334 m
	TSFC	g/kN-s	9.798	9.600
	Thrust produced	kN	94.94	94.95
Loiter	Mach, altitude	- , m	0.6 at 1,500 m	0.6 at 1,500 m
	TSFC	g/kN-s	12.175	11.929
	Thrust produced	kN	114.67	114.70

SI 4.4 Characteristics of LH_2 tank systems

Figure SI 4 shows the LH_2 tank integration with BWB aircraft for Case 1 LH_2 aircraft (semi-span). This is a generic view without any tank dimensions. For all three LH_2 aircraft cases, three fuel tanks are placed on each of the two sides of the cabin and the three fuel tanks are placed aft of the cabin. The tank dimensions and fuel volume for all three LH_2 aircraft cases are provided in Table SI 11.

Table SI 11 shows the LH_2 tank geometry and dimensions for three cases (semi-span) considered in the current work. The total fuel requirement for case 1 at the beginning of the mission is calculated iteratively to be 24.25 tonnes (341.56 m^3) in the weight sizing process, which is the highest of the three LH_2 cases because it is an unoptimized case. This means that the volume of the tank required will be the highest of the three cases. The tank is designed in a piece-wise manner as discussed in §2.5 (main paper). The radius and the length for each piece of the tapered cylinder/frustum are listed in Table SI 11. Considering the total aircraft, for case 1, the total designed tank volume is calculated to be 341.66 m^3. The weight of the total tank system is calculated to be 6,840 kg for case 1. Similarly, the total fuel requirement for case 2 at the beginning of the mission is calculated iteratively to be 23.82 tonnes (335.47 m^3) in the weight sizing process (tank dimensions shown in Table SI 11). Considering the total aircraft,

for case 2, the total designed tank volume is calculated to be 336.86 m^3. The weight of the total tank system is calculated to be 6,718 kg for case 2. Additionally, the total fuel requirement for case 3 at the beginning of the mission is calculated iteratively to be 23.35 tonnes (328.84 m^3) in the weight sizing process (tank dimensions shown in Table SI 11). Considering the total aircraft, for case 3, the total designed tank volume is calculated to be 329.32 m^3. The weight of the total tank system is calculated to be 6,586 kg for case 3.

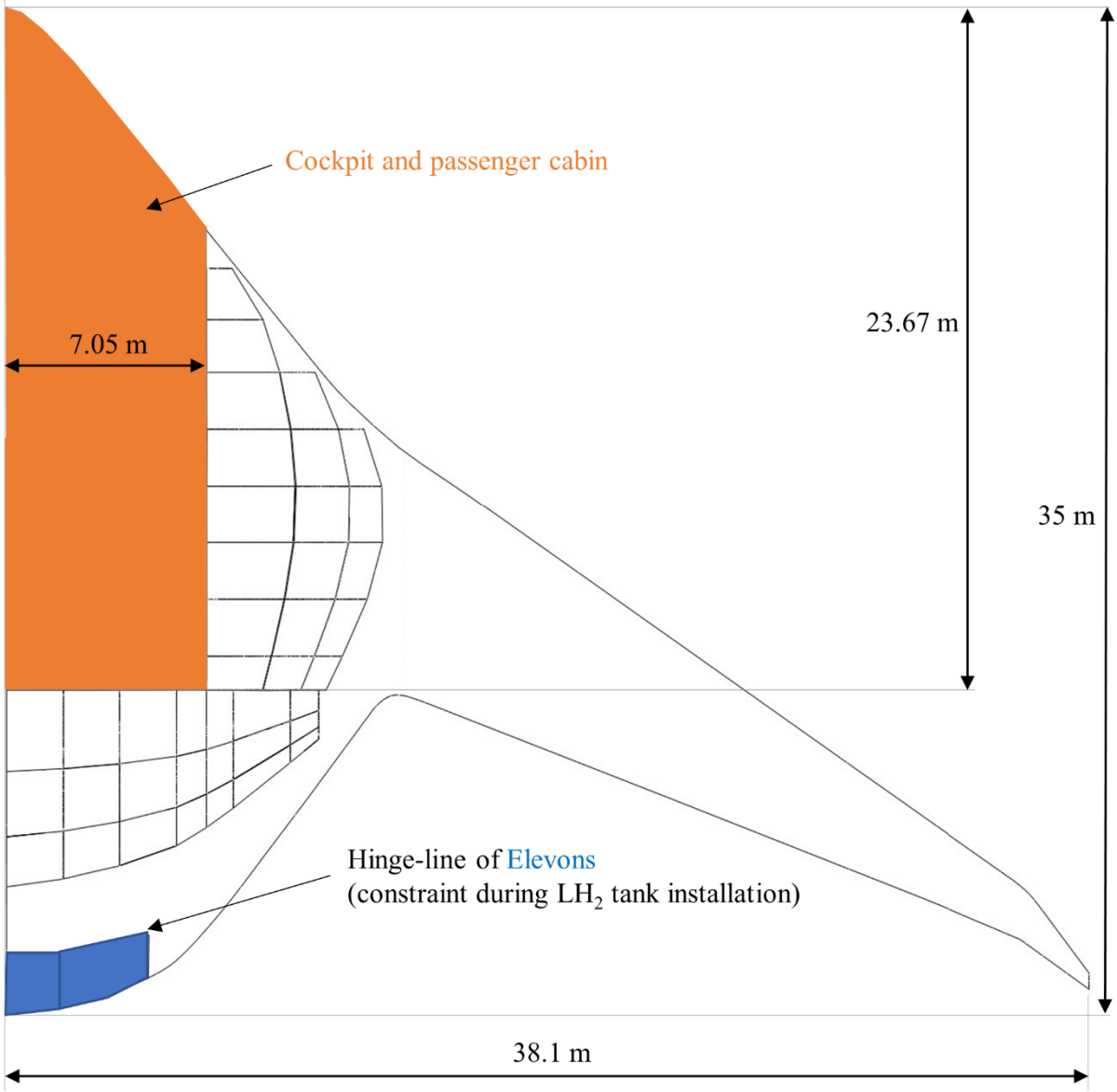

Figure SI 4. LH_2 tank integration with BWB aircraft for Case 1 LH_2 aircraft (semi-span)

Table SI 11. LH_2 tank geometry and dimensions for three cases considered in the current work

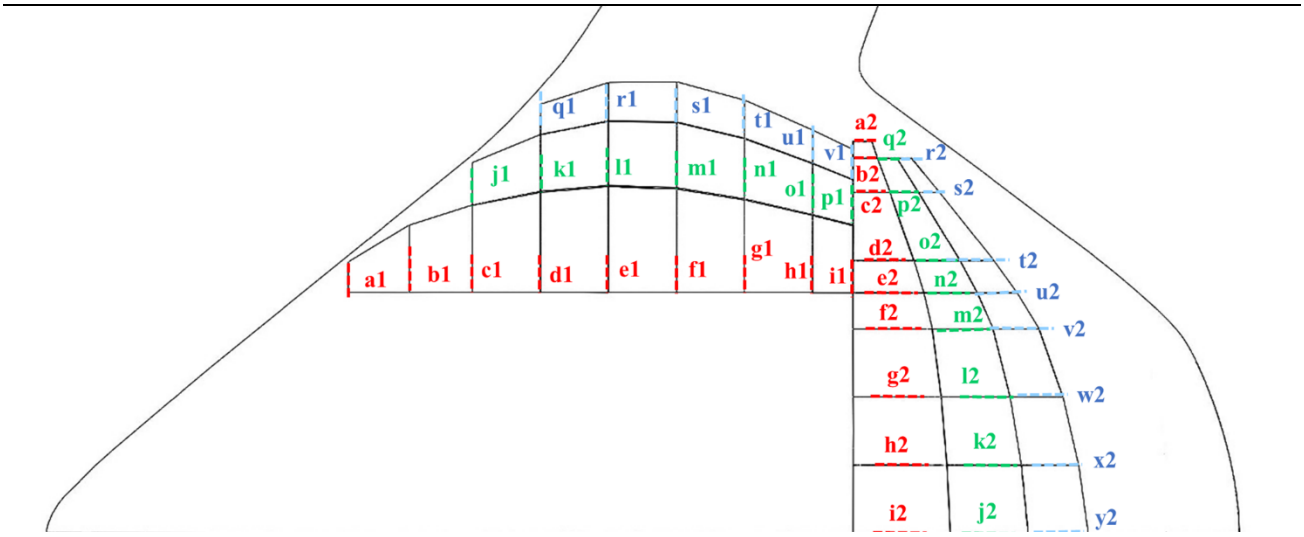

Case 1, Case 2, and Case 3 (Common tank systems to three cases)

Section	Outer radius (m)	Piece length (m)	Section	Outer radius (m)	Piece length (m)	Section	Outer radius (m)	Piece length (m)
a1	0.45	0	j1	0.6275	0	q1	0.448	0
b1	0.9975	1.8	k1	0.8485	2	r1	0.57	2
c1	1.29	1.85	l1	0.964	2	s1	0.6	2
d1	1.49	2	m1	0.9825	2	t1	0.57	2
e1	1.5775	2	n1	0.905	2	u1	0.495	2
f1	1.543	2	o1	0.765	2	v1	0.4475	1.1855
g1	1.3795	2	p1	0.675	1.1855			
h1	1.15	2						
i1	1	1.1855						

Case 1 (remaining tank systems)

Section	Outer radius (m)	Piece length (m)	Section	Outer radius (m)	Piece length (m)	Section	Outer radius (m)	Piece length (m)
a2	0.275	0	j2	1.144	0	r2	0.215	0
b2	0.36	0.5	k2	1.094	2	s2	0.31	1
c2	0.549	1	l2	1.0125	2	t2	0.5	2
d2	0.9	2	m2	0.893	2	u2	0.5895	0.95
e2	1.045	0.95	n2	0.7825	1.05	v2	0.677	1.05
f2	1.17	1.05	o2	0.674	0.95	w2	0.775	2
g2	1.3	2	p2	0.4175	2	x2	0.84	2
h2	1.385	2	q2	0.29	1	y2	0.8825	2
i2	1.435	2						

Case 2 (remaining tank systems)								
Section	Outer radius (m)	Piece length (m)	Section	Outer radius (m)	Piece length (m)	Section	Outer radius (m)	Piece length (m)
c2	0.549	0	j2	1.144	0	u2	0.5895	0
d2	0.9	2	k2	1.094	2	v2	0.677	1.05
e2	1.045	0.95	l2	1.0125	2	w2	0.775	2
f2	1.17	1.05	m2	0.893	2	x2	0.84	2
g2	1.3	2	n2	0.7825	1.05	y2	0.8825	2
h2	1.385	2	o2	0.674	0.95			
i2	1.435	2	p2	0.4175	2			
Case 3 (remaining tank systems)								
Section	Outer radius (m)	Piece length (m)	Section	Outer radius (m)	Piece length (m)	Section	Outer radius (m)	Piece length (m)
c2	0.549	0	j2	1.144	0	v2	0.677	0
d2	0.9	2	k2	1.094	2	w2	0.775	2
e2	1.045	0.95	l2	1.0125	2	x2	0.84	2
f2	1.17	1.05	m2	0.893	2	y2	0.8825	2
g2	1.3	2	n2	0.7825	1.05			
h2	1.385	2						
i2	1.435	2						

SI 4.5 Aircraft weight and fuel consumption breakdown over flight mission

Table SI 12. Fuel fractions, aircraft weight and fuel consumption over flight mission of Jet-A BWB aircraft

No.	Segment	FF -	Start weight kg	Fuel used kg
1	Engine start and warm-up	0.9964	236,398	847
2	Taxi-out	0.9964	235,551	844
3	Take-off	0.9982	234,708	420
4	Climb	0.9975	234,287	584
5	Cruise	0.7474	233,704	59,035
6	Descent and approach	0.9964	174,669	626
7	Loiter	0.9846	174,043	2,678
8	Land, taxi-in and shutdown	0.9971	171,366	491
	Total	0.72	170,875 (weight of aircraft at the end of flight mission)	$W_{F,block}$ = 65,523

Using the aircraft weight sizing process detailed in §2.5 (main paper), the aircraft weight and the fuel consumption over the flight mission are calculated for the baseline case (Jet-A BWB aircraft), 100% SPK, and three cases of LH_2 aircraft. Tables SI 12, SI 13, SI 14,

SI 15, and SI 16 provide the FFs, aircraft weight and fuel consumption over one flight mission for Jet-A BWB aircraft, case 1 (LH_2), case 2 (LH_2), case 3 (LH_2), and 100% SPK, respectively. It can be observed that the ratio of the $W_{F,block}$ of Jet-A case and case 1, 2, and 3 is 3:1, 3.06:1, and 3.13:1, respectively.

Table SI 13. Fuel fractions, aircraft weight and fuel consumption over flight mission of LH_2 case 1

No.	Segment	FF -	Start weight kg	Fuel used kg
1	Engine start and warm-up	0.9987	195,325	244
2	Taxi-out	0.9987	195,080	244
3	Take-off	0.9994	194,837	122
4	Climb	0.9991	194,715	172
5	Cruise	0.8984	194,543	19,758
6	Descent and approach	0.9987	174,786	218
7	Loiter	0.9947	174,567	932
8	Land, taxi-in and shutdown	0.9990	173,635	174
	Total	0.89	173,461 (weight of aircraft at the end of flight mission)	$W_{F,block}$ = 21,863

Table SI 14. Fuel fractions, aircraft weight and fuel consumption over flight mission of LH_2 case 2

No.	Segment	FF -	Start weight kg	Fuel used kg
1	Engine start and warm-up	0.9987	194,177	243
2	Taxi-out	0.9987	193,935	242
3	Take-off	0.9994	193,692	121
4	Climb	0.9991	193,571	170
5	Cruise	0.8998	193,401	19,384
6	Descent and approach	0.9987	174,018	218
7	Loiter	0.9947	173,800	923
8	Land, taxi-in and shutdown	0.9990	172,887	173
	Total	0.89	172,704 (weight of aircraft at the end of flight mission)	$W_{F,block}$ = 21,473

The ratio of gravimetric energy densities of LH_2 fuel and Jet-A is (120/43.2=) 2.78. The above ratio of the block fuel consumption of Jet-A aircraft and LH_2 aircraft is ~3:1 as compared to the ratio of the gravimetric energy densities of LH_2 and Jet-A of 2.78:1. This means that LH_2 aircraft design analysis, in general, cannot be just limited in terms of the effect of improved TSFC due to the use of a high gravimetric energy density fuel (like LH_2) in propulsion systems. The effect of the aircraft weight reduction (and thrust requirement reduction leading to smaller engines the resulting reduction in the engine weight) while carrying less weight of a high

gravimetric energy density fuel (like LH_2), also contributes to the above ratio of $W_{F,block}$ (of Jet-A aircraft and LH_2 aircraft) of ~3:1, though as observed the effect of improved TSFC is dominant. For 100% SPK cases (Table SI 16), $W_{F,block}$ is of similar magnitude as that of Jet-A.

Table SI 15. Fuel fractions, aircraft weight and fuel consumption over flight mission of LH_2 case 3

No.	Segment	FF -	Start weight kg	Fuel used kg
1	Engine start and warm-up	0.9987	192,677	241
2	Taxi-out	0.9987	192,436	241
3	Take-off	0.9994	192,196	120
4	Climb	0.9992	192,076	162
5	Cruise	0.9010	191,913	19,003
6	Descent and approach	0.9987	172,910	216
7	Loiter	0.9948	172,694	894
8	Land, taxi-in and shutdown	0.9990	171,800	172
	Total	0.89	171,628 (weight of aircraft at the end of flight mission)	$W_{F,block}$ = 21,049

Table SI 16. Fuel fractions, aircraft weight and fuel consumption over flight mission of 100% SPK

No.	Segment	FF -	Start weight kg	Fuel used kg
1	Engine start and warm-up	0.9965	234,798	824
2	Taxi-out	0.9965	233,974	821
3	Take-off	0.9982	233,152	409
4	Climb	0.9976	232,743	568
5	Cruise	0.7514	232,175	57,727
6	Descent and approach	0.9965	174,449	612
7	Loiter	0.9849	173,837	2,623
8	Land, taxi-in and shutdown	0.9972	171,213	481
	Total	0.73	170,733 (weight of aircraft at the end of flight mission)	$W_{F,block}$ = 64,065

SI 4.6 LH_2 BWB aircraft landing weight analysis

Considering an emergency situation, the landing weight of an aircraft is an important factor. The 'safe' landing weight is dependent on the structural weight of the aircraft. Roskam [2] recommends 0.84 to be an average permissible ratio of the aircraft landing weight and the aircraft GTOW, for a transport jet. In the event of an emergency landing immediately after take-off, the pilot performs fuel jettison or dumps the conventional jet fuel in air so that the aircraft weight goes below its permissible landing weight. However, in the case of an aircraft

powered by LH_2, this highly flammable fuel cannot be dumped into the atmosphere in events of emergency landing. Since the present work uses the same airframe/structure from the study by Nickol et al. [4] [NASA N+2 Jet-A BWB 301 passengers (PAX) aircraft], the permissible landing weight of Jet-A BWB aircraft, BWB LH_2 aircraft (all three cases), and NASA N+2 BWB 301 PAX (Jet-A) aircraft, are the same. Therefore, the GTOW of the NASA N+2 BWB 301 PAX (Jet-A) aircraft ($GTOW_{NASA}$) determines the average permissible landing weight for the said aircraft, Jet-A BWB aircraft and BWB LH_2 aircraft (all three cases). Table 2 (main paper) lists the ratio of $GTOW/GTOW_{NASA}$ for Jet-A BWB aircraft and BWB LH_2 aircraft (all three cases). It can be observed that the $GTOW/GTOW_{NASA}$ ratios for case 1, 2, and 3 of BWB LH_2 aircraft are 0.806, 0.801, and 0.795, respectively. This means that with BWB LH_2 aircraft (all three cases), there is no need to conduct fuel jettison of a highly flammable hydrogen fuel in the event of an emergency landing, because its GTOW is lower than the average permissible landing weight considering its structure. This finding is of great significance considering the safety issue associated with LH_2 use in an aircraft.

SI 4.7 Miscellaneous performance results

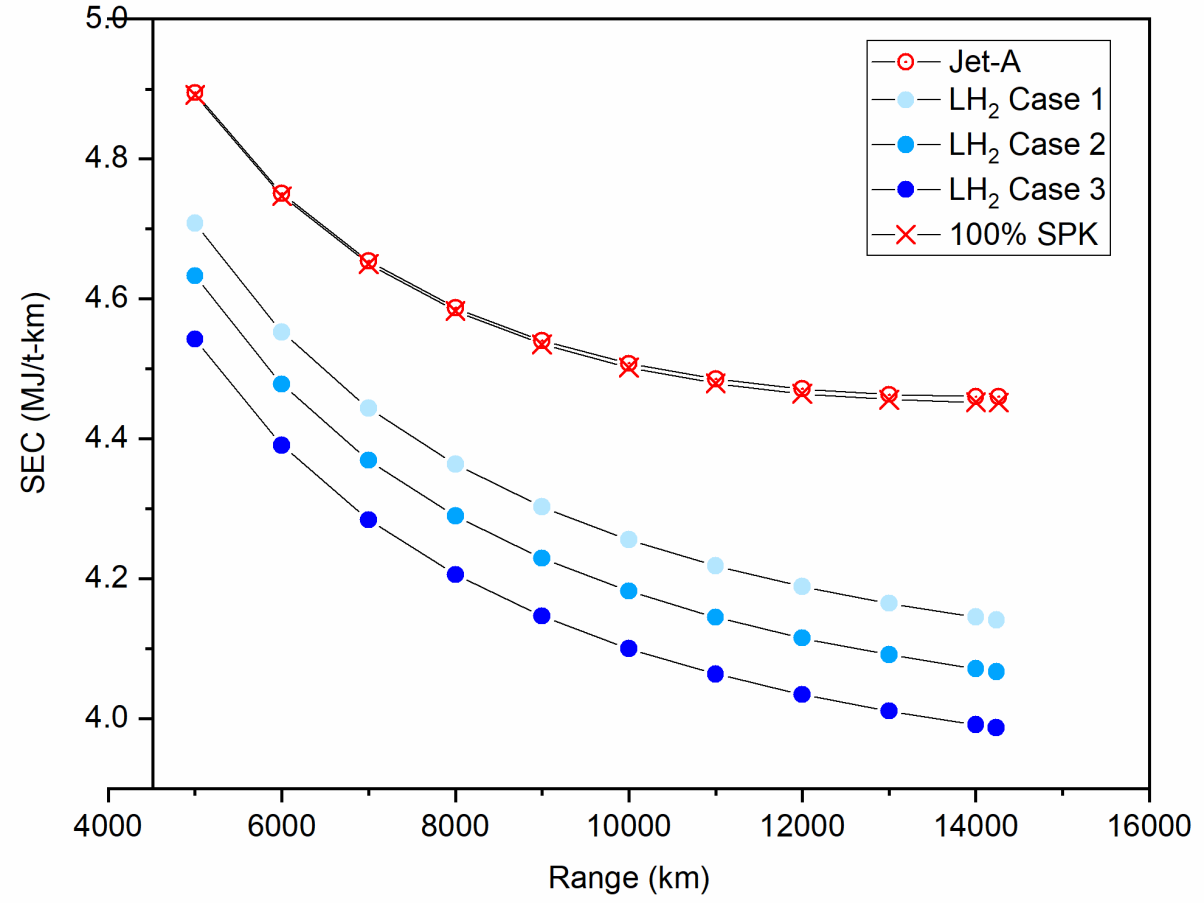

Figure SI 5. Variation of specific energy consumption (SEC) with range for BWB aircraft powered by different fuels for 83.1% load factor

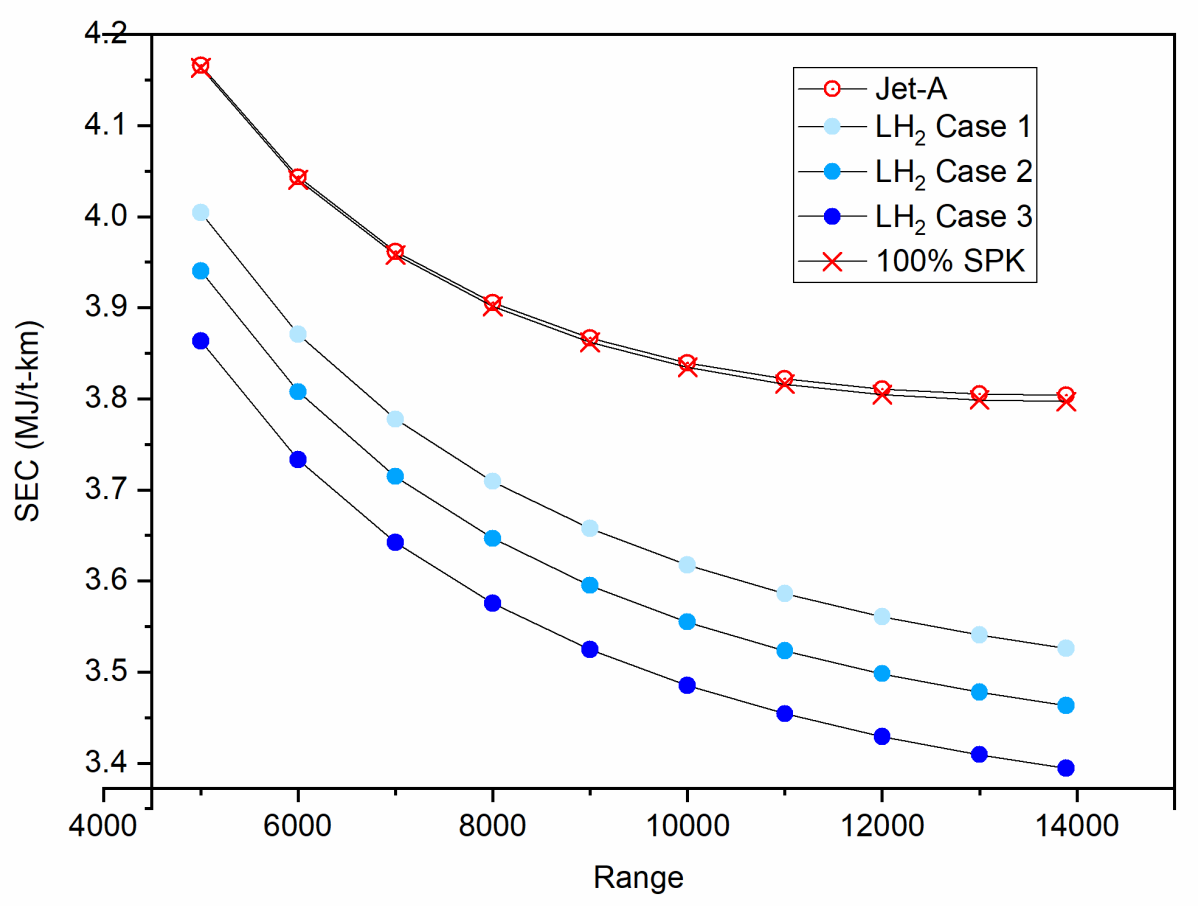

Figure SI 6. Variation of SEC with range for BWB aircraft powered by different fuels for 100% load factor

The detailed design point energy performance and aircraft characteristics of 100% SPK BWB aircraft is included in SI §4.9. Figure SI 7 shows the relationship between OEW and GTOW of aircraft in service, of future (other studies), and future aircraft designed in this work (only Jet-A and 100% SPK) (readers are advised to see Table SI 17 for source of aircraft data). It is to be noted that Figure SI 7 also includes the tube-wing [A350-1000] 100% SPK aircraft modelled in our previous study [31]. It can be observed from Figure SI 7 that the relationship between OEW and GTOW for the aircraft designed in this work is very similar to that of aircraft that have already entered in service. GTOW is an indirect measure of the structural weight of the aircraft, payload, and the fuel weight ($W_{F,block}$ and $W_{F,total}$). 100% SPK aircraft cases have similar (magnitude of) OEW and GTOW as that of BWB Jet-A case, hence these lie in the vicinity of the BWB Jet-A case. For compactness, only the names of recent aircraft in service and the aircraft designed in this work (along with reference aircraft) are mentioned in Figure SI 7.

Referring to Figure SI 7, the data points on left (GTOW< 1.0E+5), centre (1.0E+5<GTOW<4.0E+5), and right (GTOW>4.0E+5) are primarily of small aircraft (short range), LTA and small twin aisle aircraft (medium and long range), and VLTA (large quads and long range), respectively. All these data points used for creating both Figure 8 (§3.3 in the main paper) and Figure SI 7, are listed in Table SI 17. Additionally, by using the developed

equation in Figure SI 7, and knowing either OEW or GTOW, the GTOW or OEW can be estimated for low-order modelling.

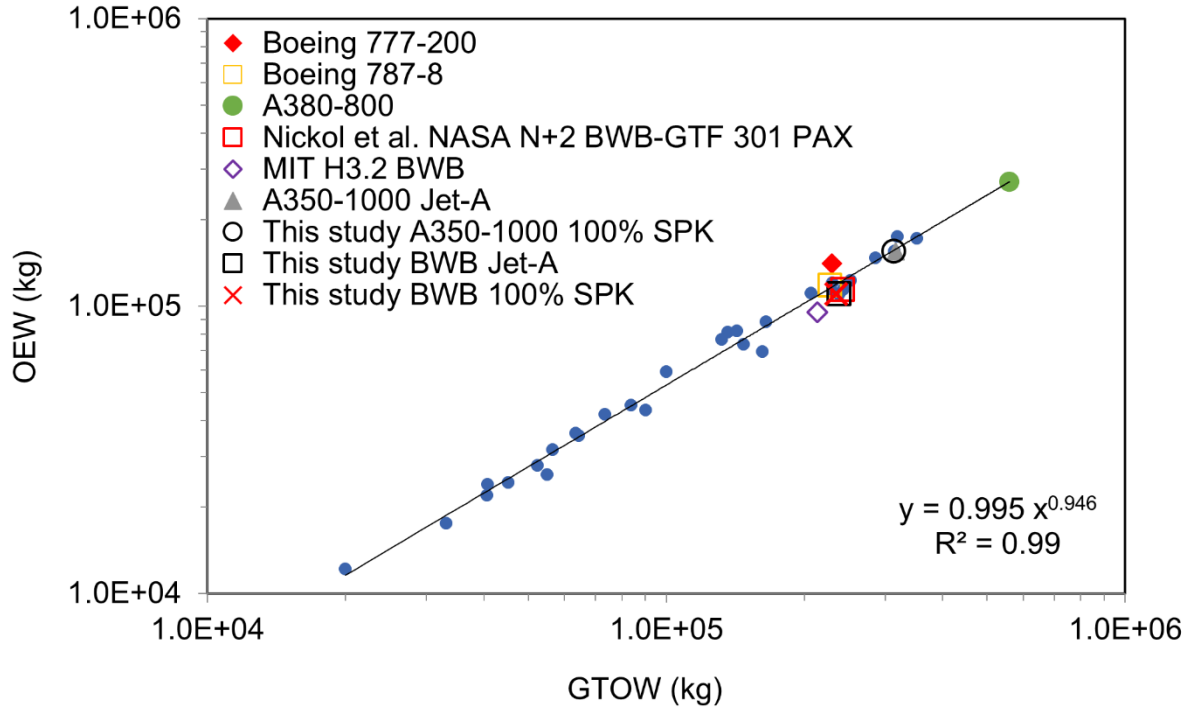

Figure SI 7. Relationship between OEW and GTOW of aircraft in service, of future (other studies) and future aircraft designed in this work (only Jet-A and 100% SPK) (see Table SI 17 for source of data)

Table SI 17. OEW and GTOW of aircraft already into service, in literature and aircraft designed in this work

Aircraft	GTOW (kg)	OEW (kg)
27 Aircraft already into service ([2,35–37])		
727-200	83,824	45,359
737-200	52,390	27,955
737-300	56,472	31,720
747-200B	351,534	172,365
747-SP	285,763	147,417
757-200	99,790	59,157
767-200	136,078	81,230
DC8-Super 71	147,417	73,799
DC9-30	54,885	25,941
DC9-80	63,503	36,177
DC10-10	206,384	111,086
DC10-40	251,744	122,952
Lockheed L1011-500	231,332	111,357
Fokker F28-4000	33,112	17,546
Rombac-111-560	45,200	24,386
VFW-Fokker 614	19,958	12,179

BAe 146-200	40,596	21,999
A300-B4-200	164,999	88,500
A310-202	131,995	76,616
Ilyushin-Il-62M	162,000	69,400
Tupolev-154	90,000	43,499
A330-200	229,998	120,499
Airbus A320	73,498	42,100
Boeing 777-200	229,518	140,659
A380-800	559,993	270,012
Boeing 787-8	227,930	117,707
A350-1000	316,000	155,129
Nine futuristic aircraft (Jet-A and 100% SPK) [4,31,38]		
Over wing nacelle 98 – direct drive engine	40,728	23,977
Over wing nacelle 160 – GTF	64,350	35,551
BWB 216 – GTF	142,364	82,169
BWB 400 – GTF	318,661	174,793
MIT H3.2 BWB	213,445	95,243
Nickol et al. NASA N+2 BWB-GTF 301 PAX	242,441	114,349
Jagtap et al. (2023) A350-1000 100% SPK	313,404	155,314
This study BWB Jet-A	237,685	110,151
This study BWB 100% SPK (see SI 4.9 for details)	234,798	110,169
54 LH_2 aircraft [17,18,31,39–61]		
Aircraft	GTOW (kg)	OEW (kg)
Jagtap et al. (2023) (366 PAX 13,870 km) tank index 0.78	2,68,516	1,83,371
Jagtap et al. (2024) N+2 (366 PAX 13,870 km) tank index 0.88	2,13,149	1,44,321
Jagtap et al. (2024) N+3 (366 PAX 13,870 km) tank index 0.88	2,08,358	1,43,155
Brewer (400 PAX 10,186 km)	1,68,740	1,03,300
Brewer (130 PAX 2,778 km)	45,510	29,780
Brewer (200 PAX 5,556 km)	79,600	51,540
Brewer (400 PAX 5,556 km)	1,43,330	90,340
Brewer (400 PAX 18,520 km)	2,49,400	1,49,840
Verstraete (150 PAX 4,000 km)	78,000	58,200
Verstraete (300 PAX 9,000 km)	1,75,700	1,22,900
Verstraete (400 PAX 14,000 km)	2,50,100	1,61,600
Troeltsch et al. (400 PAX 11,853 km)	1,96,000	1,28,000
Proesmans et al. ATR (67 PAX 2,410 km)	32,200	20,500
Proesmans et al. COC (67 PAX 2,410 km)	33,100	21,500
Proesmans et al. ATR (130 PAX 3,200 km)	63,600	41,200
Proesmans et al. COC (130 PAX 3,200 km)	64,500	42,600
Proesmans et al. ATR (253 PAX 10,800 km)	2,44,000	1,56,000
Proesmans et al. COC (253 PAX 10,800 km)	2,48,000	1,63,000
Gomez et al. (194 PAX 9,000 km)	1,33,676	1,08,897
Airbus Cryoplane (185 PAX 7,400 km)	87,600	61,200

Silberhorn et al. (2019) (165 PAX 5,740 km) Rear tank	67,819	44,334
Silberhorn et al. (2019) (165 PAX 5,740 km) Top tank	66,045	42,605
Silberhorn et al. (2019) (165 PAX 5,740 km) Pod tank	64,584	41,084
Beck et al. BWB (524 PAX 11,408 km)	2,88,994	2,01,003
Silberhorn et al. (2022) (261 PAX, 7,220 km)	1,28,670	92,245
Lammen et al. (300 PAX, 3,704 km)	1,64,900	1,28,600
Onorato et al. (72 PAX, 926 km)	22,900	14,600
Onorato et al. (150 PAX, 4,560 km)	77,000	52,000
Onorato et al. (295 PAX, 7,674 km)	2,10,000	1,41,000
Huete et al. (232 PAX, 10,370 km)	3,09,000	2,38,000
Mourouzidis et al. (332 PAX, 8,890 km) tank index 0.45	3,03,000	2,29,000
Mourouzidis et al. (332 PAX, 8,890 km) tank index 0.67	263000	1,89,000
Huete et al. (388 PAX, 6,112 km)	2,73,000	2,00,000
Huete et al. (720 PAX, 3,334 km)	2,87,000	1,94,000
Smith et al. (242 PAX, 4,250 km)	1,29,000	98,150
Karpuk et al. (~210 PAX, 4,000 km)	65,591	42,668
Karpuk et al. BWB (378 PAX, 10,580 km)	2,60,846	1,62,900
Ramm et al.	82,100	54,800
Burschyk et al. (250 PAX, 2,778 km)	69,600	43,200
Adler et al. (420 PAX, 10,186 km)	2,44,861	1,62,312
Adler et al. BWB (420 PAX, 10,186 km)	2,12,835	1,38,286
Barton et al. (108 PAX, 3,000 km) 12.5 km cruise altitude	63,000	44,000
Barton et al. (108 PAX, 3,000 km) 14 km cruise altitude	68,000	48,000
Oak et al. (132 PAX, 5,740 km)	56,426	39,592
VanLandingham et al. (~40 PAX, 1,948 km)	15,805	11,357
VanLandingham et al. (~180 PAX, 6,575 km)	75,379	50,937
Camboni (150 PAX, 3,000 km)	62282	42813
Palaia et al. (116 PAX, 7,730 km)	92,143	70,000
Palaia et al. (116 PAX, 5,990 km)	89,836	70,000
Palaia et al. (84 PAX, 9,770 km)	91,816	70,000
Palaia et al. (84 PAX, 7,810 km)	89,438	70,000
This study BWB LH_2 Case 1 (301 PAX 13,890 km)	1,96,339	1,18,194
This study BWB LH_2 Case 2 (301 PAX 13,890 km)	1,95,206	1,17,501
This study BWB LH_2 Case 3 (301 PAX 13,890 km)	1,93,732	1,16,505

SI 4.8 Weight sizing of BWB LNG aircraft

Similar to our previous study [31], two liquid natural gas (LNG) cases are considered here for BWB powered by LNG (gravimetric energy density of 50 MJ/kg and density 424 kg/m^3 [62]). The first LNG case uses a hypothetical value of $\eta = 0.78$, similar to LH_2 case. In the second LNG case, a present-day (best) value of $\eta = 0.63$ is used, which is similar to the values used in transportation of LNG fuel via trucks [63]. In the LNG BWB aircraft weight sizing process, similar process schematic (Figure 2 of main paper) and methodology discussed in §2.5 are used for both LNG cases, as that used for (same thrust requirement) LH_2 case 1

(LNG has similar gravimetric energy density on the order of Jet-A but has approximately half the Jet-A fuel density). This is based on the finding of our previous study [31]. For both LNG cases, the fuel will be stored in the volume available as per the tanks designed for LH_2 case 1 in BWB wings, which has the maximum fuel volume storage requirement. The FF for Jet-A and both LNG cases are calculated according to the methodology discussed in SI §3.3, and these are listed in Table SI 18. The propulsion system is designed according to the methodology detailed in [26] using GasTurb 13. Table SI 19 lists the performance of propulsion system at different points in the flight mission profile for Jet-A and LNG (two cases) and their weights.

Table SI 18. FFs for Jet-A, and FFs for LNG cases

Segment	Operation	Modified FFs (Jet-A)	FFs (LNG case 1)	FFs (LNG case 2)
1	Engine start and warmup	0.9964	0.9969	0.9969
2	Taxi-out	0.9964	0.9969	0.9969
3	Take-off	0.9982	0.9985	0.9985
4	Climb	0.9975	0.9979	0.9979
5	Cruise	0.7474	0.8504	0.8077
6	Descent	0.9964	0.9969	0.9969
7	Loiter	0.9846	0.9881	0.9879
8	Land, taxi-in, engine shutdown	0.9971	0.9975	0.9975
	Overall FF	0.72	0.83	0.79

Table SI 19. Performance of propulsion system at different points in the flight mission profile for Jet-A and LNG (two cases) and their weights

		Units	Jet-A	LNG case 1	LNG case 2
Total propulsion systems weight		kg	12,319	12,319	12,319
TOC	Mach, altitude	- , m	0.8 at 10,668 m	0.8 at 10,668 m	0.8 at 10,668 m
	TSFC	g/kN-s	12.400	10.669	10.669
Cruise	Mach, altitude	- , m	0.84 at 10,668 m	0.84 at 10,668 m	0.84 at 10,668 m
	TSFC	g/kN-s	12.667	10.898	10.898
SLS	Mach, altitude	- , m	0 at 0 m	0 at 0 m	0 at 0 m
	TSFC	g/kN-s	5.124	4.409	4.409
Climb	Mach, altitude	- , m	0.47 at 5,334 m	0.47 at 5,334 m	0.47 at 5,334 m
	TSFC	g/kN-s	9.798	8.430	8.430
Loiter	Mach, altitude	- , m	0.6 at 1,500 m	0.6 at 1,500 m	0.6 at 1,500 m
	TSFC	g/kN-s	12.175	10.475	10.475

Table SI 20 provides a comparison of BWB aircraft performance powered by Jet-A, LH_2, and LNG (both cases). The effect of LNG cryogenic tank η can be observed from Table SI 20. With increasing η, the aircraft range and $W_{F,total}$ increases, and the OEW decreases. This is similar to the observation made in our previous study [31] for tube-wing LNG aircraft. For both LNG cases, the GTOW = maximum take-off weight (MTOW) (of BWB Jet-A structure) during the weight sizing process. Both BWB LNG cases do not meet the design target range as

the GTOW = MTOW and the weight sizing process ends, and no more fuel can be added to the aircraft. For LNG case 1 which has highest cryogenic tank η of the two cases, the aircraft reaches a range of 12,052 km. Therefore, LNG is not identified as an alternative fuel for use in a future N+2 BWB aircraft (since target design range is not met).

Table SI 20. Comparison of BWB aircraft performance powered by Jet-A, LH_2, and LNG (both cases)

BWB	Cryogenic tank η	GTOW (kg)	OEW (kg)	$OEW/GTOW_{Jet\text{-}A}$	$W_{F,total}$ (kg)	$W_{F,block}$ (kg)	Cryogenic tank volume (m^3)	Range (km)
Jet-A	-	236,398	110,150	0.466	72,678	65,523	-	13,890
LNG C1	0.78	236,398	126,588	0.535	56,241	50,704	132.65	*12,052*
LNG C2	0.63	236,398	137,591	0.582	45,238	40,784	106.7	*9,263*
LH_2 C1	0.78	195,325	117,505	0.497	24,250	21,863	341.6	13,890
LH_2 C2	0.78	194,177	116,790	0.494	23,818	21,473	335.5	13,890
LH_2 C3	0.78	192,677	115,760	0.49	23,348	21,049	329	13,890
100% SPK	-	234,798	110,169	0.466	71,061	64,065	-	13,890

SI 4.9 Weight sizing of BWB 100% SPK aircraft

Table SI 21 provides the performance comparison of Boeing 777-200 LR and future aircraft (Jet-A BWB aircraft and BWB 100% SPK aircraft) over one flight mission. BWB 100% SPK aircraft has similar performance metrics as that of BWB Jet-A aircraft. BWB 100% SPK case has insignificant energy efficiency improvement of 0.19%. This is similar to the findings of Hileman et al. [64] (0.3% improvement in energy efficiency), Proesmans et al. [57] (similar energy consumption), and that of our previous study [31] (0.17%), for a tube-wing aircraft. Additionally, for the 100% SPK BWB aircraft there is an insignificant increase in the OEW (of 19 kg in fuel tank weight) to accommodate slightly less mass-dense (100% SPK) fuel than Jet-A. It is to be noted that 100% SPK is not a drop-in fuel presently.

Table SI 21. Performance comparison of Boeing 777-200 LR and future aircraft [Jet-A BWB aircraft and BWB 100% SPK aircraft] over one flight mission

Aircraft range: 13,890 km (Current scenario)				
Aircraft			Jet-A block fuel consumption (kg)	Jet-A block fuel energy consumption (TJ)
Boeing 777-200LR			125,705	5.43
Aircraft range: 13,890 km (Future scenarios)				
Parameters	Units	Nickol et al. [4]	Jet-A BWB aircraft	BWB 100% SPK aircraft
GTOW	kg	242,441	236,398	234,798
OEW	kg	114,907	110,150	110,169
Payload weight	kg	53,570	53,570	53,570
$W_{F,total}$	kg	73,965	72,678	71,059
GTOW / $GTOW_{NASA}$	-	1	0.975	0.968
$W_{F,block}$	kg	66,683	65,523	64,065
Block fuel energy	TJ	2.88	2.83	2.82
Block fuel energy reduction as compared to Boeing 777-200LR	%	47%	47.88%	47.97%
Block fuel energy reduction as compared to Jet-A BWB aircraft	%		-	0.187%
(*L/D*) at cruise	-	23.7	23.7	23.656
Block fuel weight/total fuel weight	-	0.9	0.9	0.9
T/W (SLS)	-	0.252	0.262	0.264
T/W (TOC)	-	-	0.04851	0.04883
Structurally (average) permissible ratio of aircraft landing weight and GTOW, for transport jet			0.84 (according to Roskam [2])	

More information:

First author's other research work can be found in [17,26,31,65–86,90–95].

References

[1] Raymer D. Aircraft Design: A Conceptual Approach, Sixth Edition. Washington, DC: American Institute of Aeronautics and Astronautics, Inc.; 2018. https://doi.org/10.2514/4.104909.

[2] Roskam J. Airplane Design. Part I: Preliminary Sizing of Airplanes. DAR Corporation; 2005.

[3] Kundu AK, Price MA, Riordan D. Conceptual Aircraft Design : an Industrial Perspective. First. John Wiley & Sons, Incorporated; 2019.

[4] Nickol CL, Haller WJ. Assessment of the Performance Potential of Advanced Subsonic Transport Concepts for NASA's Environmentally Responsible Aviation Project. 54th AIAA Aerosp. Sci. Meet., Reston, Virginia: American Institute of Aeronautics and Astronautics; 2016. https://doi.org/10.2514/6.2016-1030.

[5] Quinlan JR, Gern FH. Conceptual design and structural optimization of nasa environmentally responsible aviation (ERA) hybrid wing body aircraft. 57th AIAA/ASCE/AHS/ASC Struct. Struct. Dyn. Mater. Conf., American Institute of Aeronautics and Astronautics; 2016. https://doi.org/10.2514/6.2016-0229.

[6] Verstraete D. Long range transport aircraft using hydrogen fuel. Int J Hydrogen Energy 2013;38:14824–31. https://doi.org/10.1016/j.ijhydene.2013.09.021.

[7] Nickol CL. Hybrid wing body configuration scaling study. 50th AIAA Aerosp. Sci. Meet. Incl. New Horizons Forum Aerosp. Expo., Nashville, Tennessee: 2012. https://doi.org/10.2514/6.2012-337.

[8] Thomas RH, Burley CL, Nickol CL. Assessment of the Noise Reduction Potential of Advanced Subsonic Transport Concepts for NASA's Environmentally Responsible Aviation Project. 54th AIAA Aerosp. Sci. Meet., Reston, Virginia: American Institute of Aeronautics and Astronautics; 2016. https://doi.org/10.2514/6.2016-0863.

[9] Nickol CL, McCullers LA. Hybrid Wing body configuration system studies. 47th AIAA Aerosp. Sci. Meet. Incl. New Horizons Forum Aerosp. Expo., Orlando, Florida: 2009. https://doi.org/10.2514/6.2009-931.

[10] Nickol CL. Technologies and Concepts for Reducing the Fuel Burn of Subsonic Transport Aircraft. NTRS - NASA Tech Reports Serv 2012. https://ntrs.nasa.gov/citations/20120016006 (accessed September 3, 2020).

[11] Goraj Z. Design and Optimisation of Fuel Tanks for BWB Configurations. Arch Mech Eng 2016;63:605–17. https://doi.org/10.1515/meceng-2016-0034.

[12] Khandelwal B, Karakurt A, Sekaran PR, Sethi V, Singh R. Hydrogen powered aircraft: The future of air transport. Prog Aerosp Sci 2013;60:45–59. https://doi.org/10.1016/j.paerosci.2012.12.002.

[13] Verstraete D, Hendrick P, Pilidis P, Ramsden K. Hydrogen fuel tanks for subsonic transport aircraft. Int J Hydrogen Energy 2010;35:11085–98. https://doi.org/10.1016/j.ijhydene.2010.06.060.

[14] CleanSky2-FCH. Hydrogen-powered aviation. CleanSky2 - Fuel Cell Hydrog 2020. https://doi.org/10.2843/766989.

[15] Winnefeld C, Kadyk T, Bensmann B, Krewer U, Hanke-Rauschenbach R. Modelling and Designing Cryogenic Hydrogen Tanks for Future Aircraft Applications. Energies 2018;11:105. https://doi.org/10.3390/en11010105.

[16] Verstraete D. The Potential of Liquid Hydrogen for long range aircraft propulsion. Cranfield University; 2009.

[17] Jagtap SS, Childs PRN, Stettler MEJ. Performance sensitivity of subsonic liquid hydrogen long-range tube-wing aircraft to technology developments. Int J Hydrogen Energy 2024;50:820–33. https://doi.org/10.1016/J.IJHYDENE.2023.07.297.

[18] Beck R, Bieler J, Borsutzki S, Cabac Y, Dehmel J, Khosravi R, et al. Efficiency meets sky. Jt NASA/DLR Aeronaut Des Chall 2017-18 2018. https://www.dlr.de/dlr/Portaldata/1/Resources/documents/2018/TU_Berlin_EFFICIENCY_MEETS_SKY.pdf (accessed January 19, 2020).

[19] Polek G. HyPoint Extends Hydrogen Flight Range with New Ultralight Fuel Tanks. FutureFlight 2022. https://www.futureflight.aero/news-article/2022-03-29/hypoint-extends-hydrogen-flight-range-new-ultralight-fuel-tanks (accessed July 22, 2022).

[20] Sjöberg J, Smith J, Haglund Nilsson O, Emanuelsson P, Otlu S. Liquid Hydrogen Tanks for Low-Emission Aircraft. Chalmers University of Technology, 2021.

[21] Garmendia DC. A MULTI-DISCIPLINARY CONCEPTUAL DESIGN METHODOLOGY FOR ASSESSING CONTROL AUTHORITY ON A HYBRID WING BODY CONFIGURATION. Georgia Institute of Technology; 2015.

[22] LOCKHEED C-5A BL488.2 AIRFOIL (c5b-il) n.d. http://airfoiltools.com/airfoil/details?airfoil=c5b-il (accessed September 2, 2020).

[23] KC-135 BL52.44 AIRFOIL (kc135a-il) n.d. http://airfoiltools.com/airfoil/details?airfoil=kc135a-il (accessed September 2, 2020).

[24] BOEING-VERTOL VR-15 AIRFOIL (vr15-il) n.d. http://airfoiltools.com/airfoil/details?airfoil=vr15-il (accessed September 2, 2020).

[25] June JC, Thomas RH, Guo Y. System Noise Prediction Uncertainty Quantification for a Hybrid Wing–Body Transport Concept. AIAA J 2020;58:1157–70. https://doi.org/10.2514/1.J058226.

[26] Jagtap SS, Childs PRN, Stettler MEJ. Conceptual design-optimisation of a future hydrogen-powered ultrahigh bypass ratio geared turbofan engine. Int J Hydrogen Energy 2024;95:317–28. https://doi.org/10.1016/J.IJHYDENE.2024.10.329.

[27] Seeckt K. Aircraft Preliminary Sizing with PreSTo Re-Design of the Boeing B777-200LR Aircraft Preliminary Sizing with PreSTo. 2008.

[28] Obert E. Aerodynamic Design of Transport Aircraft. 2009.

[29] RAeS. Air Travel - Greener by Design The Technology Challenge, Report of the Technology Sub-Group. 2003.

[30] Kenway G, Henderson R, Hicken J, Kuntawala N, Zingg D, Martins J, et al. Reducing Aviation's Environmental Impact Through Large Aircraft for Short Ranges. 48th AIAA Aerosp. Sci. Meet. Incl. New Horizons Forum Aerosp. Expo., Reston, Virigina: American Institute of Aeronautics and Astronautics; 2010.

https://doi.org/10.2514/6.2010-1015.

[31] Jagtap SS, Childs PRN, Stettler MEJ. Energy performance evaluation of alternative energy vectors for subsonic long-range tube-wing aircraft. Transp Res Part D Transp Environ 2023;115:103588. https://doi.org/10.1016/J.TRD.2022.103588.

[32] Boeing 767 Aircraft Operations 2013. https://studylib.net/doc/18499334/delta-virtual-airlines-boeing-767-aircraft-operations (accessed January 25, 2019).

[33] Kurzke J. GasTurb 13. GasTurb GmbH 2017. https://gasturb.de/software/gasturb.html.

[34] Pereira SR, Fontes T, Coelho MC. Can hydrogen or natural gas be alternatives for aviation? - A life cycle assessment. Int. J. Hydrogen Energy, vol. 39, Elsevier Ltd; 2014, p. 13266–75. https://doi.org/10.1016/j.ijhydene.2014.06.146.

[35] Jackson PA. IHS Jane's all the world's aircraft : development & production. Janes Information Group; 2014.

[36] Airbus. A350 AIRCRAFT CHARACTERISTICS AIRPORT AND MAINTENANCE PLANNING. Airbus 2020. https://www.airbus.com/sites/g/files/jlcbta136/files/2021-11/Airbus-Commercial-Aircraft-AC-A350-900-1000.pdf.

[37] Medium.com. Boeing 777X: Dimensions matter. MediumCom 2017. https://medium.com/o530-carris-pt-herald/boeing-777x-dimensions-matter-8e80dd601a83 (accessed August 27, 2020).

[38] Greitzer EM, Bonnefoy PA, De la Rosa Blanco E, Dorbian CS, Drela M, Hall DK, et al. N+3 Aircraft Concept Designs and Trade Studies, Final Report, Volume 1. 2010.

[39] Troeltsch F, Engelmann M, Peter F, Kaiser J, Hornung M, Scholz AE. Hydrogen powered long haul aircraft with minimized climate impact. AIAA Aviat 2020 FORUM 2020:14. https://doi.org/10.2514/6.2020-2660.

[40] Onorato G, Proesmans P, Hoogreef MFM. Assessment of hydrogen transport aircraft: Effects of fuel tank integration. CEAS Aeronaut J 2022;1:1–33. https://doi.org/10.1007/S13272-022-00601-6/TABLES/11.

[41] Mourouzidis C, Singh G, Sun X, Huete J, Nalianda D, Nikolaidis T, et al. Abating CO2 and non-CO2 emissions with hydrogen propulsion. Aeronaut J 2024:1–18. https://doi.org/10.1017/AER.2024.20.

[42] Huete J, Nalianda D, Pilidis P. Propulsion system integration for a first-generation hydrogen civil airliner? Aeronaut J 2021;125:1654–65. https://doi.org/10.1017/AER.2021.36.

[43] Huete J, Nalianda D, Pilidis P. Impact of tank gravimetric efficiency on propulsion system integration for a first-generation hydrogen civil airliner. Aeronaut J 2022;126:1324–32. https://doi.org/10.1017/AER.2022.60.

[44] Smith JR, Mastorakos E. An energy systems model of large commercial liquid hydrogen aircraft in a low-carbon future. Int J Hydrogen Energy 2023. https://doi.org/10.1016/J.IJHYDENE.2023.04.039.

[45] Karpuk S, Elham A. Comparative study of hydrogen and kerosene commercial aircraft with advanced airframe and propulsion technologies for more sustainable aviation. Https://DoiOrg/101177/09544100221144342 2022;237:2074–91.

https://doi.org/10.1177/09544100221144342.

[46] Karpuk S, Ma Y, Elham A. Design Investigation of Potential Long-Range Hydrogen Combustion Blended Wing Body Aircraft with Future Technologies. Aerosp 2023, Vol 10, Page 566 2023;10:566. https://doi.org/10.3390/AEROSPACE10060566.

[47] Ramm J, Pohya AA, Wicke K, Wende G. Uncertainty quantification in hydrogen tank exchange: Estimating maintenance costs for new aircraft concepts. Int J Hydrogen Energy 2024;68:159–69. https://doi.org/10.1016/J.IJHYDENE.2024.04.157.

[48] Burschyk T, Cabac Y, Silberhorn D, Boden B, Nagel B. Liquid hydrogen storage design trades for a short-range aircraft concept. CEAS Aeronaut J 2023;14:879–93. https://doi.org/10.1007/S13272-023-00689-4/FIGURES/15.

[49] Adler EJ, Martins JRRA. Blended Wing Body Configuration for Hydrogen-Powered Aviation. Https://DoiOrg/102514/1C037582 2024:1–15. https://doi.org/10.2514/1.C037582.

[50] Barton DI, Hall CA, Oldfield MK. Design of a Hydrogen Aircraft for Zero Persistent Contrails. Aerosp 2023, Vol 10, Page 688 2023;10:688. https://doi.org/10.3390/AEROSPACE10080688.

[51] Oak M, Fabre A, Delavenne M, Van EN, Benard E, Defoort S. Spectral project - application of FAST-OAD code to the conceptual design of a hydrogen fuelled commercial aircraft. IOP Conf Ser Mater Sci Eng 2022;1226:012027. https://doi.org/10.1088/1757-899X/1226/1/012027.

[52] VanLandingham A, Hall DK. Conceptual Design Optimization of Liquid-Hydrogen-Fueled Transport Aircraft for Environmental and Economic Performance 2023. https://doi.org/10.2514/6.2023-3228.

[53] Camboni S. Conceptual design and operating costs estimation of a subsonic airliner powered by liquid hydrogen 2023.

[54] Palaia G, Salem KA, Carrera E. Preliminary Performance Analysis of Medium-Range Liquid Hydrogen-Powered Box-Wing Aircraft. Aerosp 2024, Vol 11, Page 379 2024;11:379. https://doi.org/10.3390/AEROSPACE11050379.

[55] Brewer GD. Hydrogen aircraft technology. CRC Press; 2017. https://doi.org/10.1201/9780203751480.

[56] Verstraete D. On the energy efficiency of hydrogen-fuelled transport aircraft. Int J Hydrogen Energy 2015;40:7388–94. https://doi.org/10.1016/j.ijhydene.2015.04.055.

[57] Proesmans P-J, Vos R. Comparison of Future Aviation Fuels to Minimize the Climate Impact of Commercial Aircraft 2022. https://doi.org/10.2514/6.2022-3288.

[58] Silberhorn D, Atanasov G, Walther J-N, Zill T. ASSESSMENT OF HYDROGEN FUEL TANK INTEGRATION AT AIRCRAFT LEVEL. Inst Transp Res 2019.

[59] Gomez A, Smith H. Liquid hydrogen fuel tanks for commercial aviation: Structural sizing and stress analysis. Aerosp Sci Technol 2019;95:105438. https://doi.org/10.1016/j.ast.2019.105438.

[60] Silberhorn D, Dahlmann K, Görtz A, Linke F, Zanger J, Rauch B, et al. Climate Impact Reduction Potentials of Synthetic Kerosene and Green Hydrogen Powered

Mid-Range Aircraft Concepts. Appl Sci 2022, Vol 12, Page 5950 2022;12:5950. https://doi.org/10.3390/APP12125950.

[61] Lammen WF, Peerlings B, Sman ES van der, Kos J. Hydrogen-powered propulsion aircraft: conceptual sizing and fleet level impact analysis. Netherlands Aerosp Cent NLR 2022. http://hdl.handle.net/10921/1587 (accessed October 7, 2022).

[62] Bicer Y, Dincer I. Life cycle evaluation of hydrogen and other potential fuels for aircrafts. Int J Hydrogen Energy 2017;42:10722–38. https://doi.org/10.1016/j.ijhydene.2016.12.119.

[63] Wessington-Cryogenics. ISO VAC 40 LNG : 40 ft LNG Iso Container. Wessingt Cryog 2020. https://wessingtoncryogenics.com/products/liquefied-natural-gas-containers/iso-vac-40-lng/ (accessed September 15, 2021).

[64] Hileman JI, Donohoo PE, Stratton RW. Energy Content and Alternative Jet Fuel Viability. J Propuls Power 2010;26:1184–96. https://doi.org/10.2514/1.46232.

[65] Jagtap SS. Comparative assessment of manufacturing setups for blended sugar-to-aviation fuel production from non-food feedstocks for green aviation. AIAA Propuls. Energy 2019 Forum, Indianapolis, Indiana: American Institute of Aeronautics and Astronautics; 2019. https://doi.org/10.2514/6.2019-4332.

[66] Jagtap SS. A heat recovery system designed for shaft-powered aircraft gas turbine engines, 2016.

[67] Emerson BL, Jagtap S, Lieuwen TC. Stability Analysis of Reacting Wakes: Flow and Density Asymmetry Effects. 53rd AIAA Aerosp. Sci. Meet., Reston, Virginia: American Institute of Aeronautics and Astronautics; 2015. https://doi.org/10.2514/6.2015-0429.

[68] Jagtap SS. Systems evaluation of subsonic hybrid-electric propulsion concepts for NASA N+3 goals and conceptual aircraft sizing. Int J Automot Mech Eng 2019;16:7259–7286. https://doi.org/https://doi.org/10.15282/ijame.16.4.2019.07.0541.

[69] Jagtap SS. A heat recovery system for shaft-driven aircraft gas turbine engines, 2014.

[70] Jagtap SS. Assessment of feedstocks for blended alcohol-to-jet fuel manufacturing from standalone and distributed scheme for sustainable aviation. AIAA Propuls. Energy 2019 Forum, Indianapolis, Indiana: American Institute of Aeronautics and Astronautics; 2019. https://doi.org/10.2514/6.2019-3887.

[71] Jagtap SS. Evaluation of blended Fischer-Tropsch jet fuel feedstocks for minimizing human and environmental health impacts of aviation. AIAA Propuls. Energy 2019 Forum, Indianapolis, Indiana: American Institute of Aeronautics and Astronautics; 2019. https://doi.org/10.2514/6.2019-4412.

[72] Jagtap SS. Evaluation of technology and energy vector combinations for decarbonising future subsonic long-range aircraft. Imperial College London, n.d.

[73] Jagtap SS, Stettler MEJ, Childs PRN. Data in brief: Performance sensitivity of subsonic liquid hydrogen long-range tube-wing aircraft to technology developments n.d.

[74] Jagtap SS, Stettler MEJ, Childs PRN. Data in brief: Conceptual design-optimisation of futuristic hydrogen powered ultrahigh bypass ratio geared turbofan engine n.d.

[75] Jagtap SS, Stettler MEJ, Childs PRN. Data in brief: Conceptual design-optimisation of a subsonic hydrogen-powered long-range blended-wing-body aircraft n.d.

[76] Jagtap SS. Aero-thermodynamic analysis of space shuttle vehicle at re-entry. IEEE Aerosp Conf Proc 2015;2015-June. https://doi.org/10.1109/AERO.2015.7119253.

[77] Jagtap S, Bhandari S. Solar Refrigeration. Sardar Patel Int Conf 2012.

[78] Jagtap S, Bhandari S. Solar Refrigeration using Triple Fluid Vapor Absorption Refrigeration and Organic Rankine Cycle. Sardar Patel Int. Conf. SPICON 2012 Mech., 2012.

[79] Komerath N, Jagtap S, Hiremath N. Aerothermoelastic Tailoring for Waveriders. US Air Force Summer Fac. Fellowsh. Progr., 2014.

[80] Jagtap SS. Exploration of sustainable aviation technologies and alternative fuels for future inter-continental passenger aircraft n.d.

[81] Jagtap SS. Identification of sustainable technology and energy vector combinations for future inter-continental passenger aircraft n.d.

[82] Jagtap SS. Heat recuperation system for the family of shaft powered aircraft gas turbine engines. US10358976B2, 2019.

[83] Jagtap SS. Heat recovery system for shaft powered aircraft gas turbine engines n.d.

[84] Jagtap SS, Bhandari S. Systems design and experimental study of a solar parabolic trough for solar refrigeration n.d.

[85] Jagtap SS. An Apparatus for Exchanging Heat with Flow in an Annulus. J Eng Sci Technol Rev 2017;10:173–6.

[86] Jagtap SS. Conceptual aircraft sizing using systems engineering for N+3 subsonic hybrid-electric propulsion concepts n.d.

[87] Jagtap SS, Childs PRN, Stettler MEJ. Data in brief: Comparing alternative fuels for a futuristic subsonic long-range aircraft on a life cycle basis 2025.

[88] Jagtap SS, Childs PRN, Stettler MEJ. Comparing alternative fuels for a futuristic subsonic long-range aircraft on a life cycle basis 2025.

[89] Jagtap SS, Childs PRN, Stettler MEJ. Comparative life cycle evaluation of alternative fuels for a futuristic subsonic long-range aircraft. Sustain Prod Consum 2025.

[90] Jagtap SS, Stettler MEJ, Childs PRN. Data in brief: Energy performance evaluation of alternative energy vectors for subsonic intercontinental tube-wing aircraft n.d.

[91] Jagtap S, Strehlow A, Reitz M, Kestler S, Cinar G. Model-Based Systems Engineering Approach for a Systematic Design of Aircraft Engine Inlet. AIAA SCITECH 2025 Forum, 2025. https://doi.org/https://doi.org/10.2514/6.2025-1410.

[92] Jagtap SS. Non-food feedstocks comparison for renewable aviation fuel production towards environmentally and socially responsible aviation. 2019 AIAA Propuls. Energy Forum, Indianapolis: American Institute of Aeronautics and Astronautics; 2019.

[93] Emerson B, Jagtap S, Quinlan JM, Renfro MW, Cetegen BM, Lieuwen T. Spatio-temporal linear stability analysis of stratified planar wakes: Velocity and density asymmetry effects. Phys Fluids 2016;28:045101. https://doi.org/10.1063/1.4943238.

[94] Jagtap SS, Childs PRN, Stettler MEJ. Conceptual design-optimisation of a subsonic hydrogen-powered long-range blended-wing-body aircraft. Int J Hydrogen Energy 2024;96:639–51. https://doi.org/10.1016/J.IJHYDENE.2024.11.331.

[95] Jagtap SS. Sustainability assessment of hydro-processed renewable jet fuel from algae from market-entry year 2020: Use in passenger aircrafts. 16th AIAA Aviat. Technol. Integr. Oper. Conf., Reston, Virginia: American Institute of Aeronautics and Astronautics; 2016. https://doi.org/10.2514/6.2016-4367.